HEP-17-0541 (R2)

Nuclear lamina genetic variants, including a truncated LAP2, in twins and siblings with nonalcoholic fatty liver disease

Graham F. Brady[1,#], Raymond Kwan[1], Peter J. Ulintz[2], Phirum Nguyen[4], Shirin Bassirian[4], Venkatesha Basrur[2], Alexey I. Nesvizhskii[2,3], Rohit Loomba[4], M. Bishr Omary[1]

[1]Department of Molecular and Integrative Physiology and Department of Internal Medicine, [2]Department of Computational Medicine and Bioinformatics, [3]Department of Pathology, University of Michigan; [4]NAFLD Research Center, Division of Gastroenterology, Department of Medicine, University of California, San Diego

#To whom correspondence should be addressed: University of Michigan Medical School, Division of Gastroenterology, Department of Internal Medicine, 1137 Catherine St., Ann Arbor, MI 48109-5622. Email: gfbrady@med.umich.edu

Keywords: steatosis; lipodystrophy; laminopathy; nucleus; genetics

Abbreviations: **ALT**, alanine aminotransferase; **DAPI**, 4',6-diamidino-2-phenylindole; **GFP**, green fluorescent protein; **IF**, intermediate filament proteins; **LAP2**, lamina-associated polypeptide 2; **MAF**, minor allele frequency; **MRE**, magnetic resonance elastography; **MRI**, magnetic resonance imaging; **MRI-PDFF**, MRI-determined proton-density fat-fraction; **NAFLD**, nonalcoholic fatty liver disease; **PAGE,** polyacrylamide gel electrophoresis; **TMPO,** thymopoietin.

Potential conflict of interest: None to report.

Financial Support: The work was supported by National Institutes of Health (NIH) grant R01 DK47918 (M.B.O.); NIH training grant T32 DK094775 (G.F.B.); American Liver Foundation (ALF) Liver Scholar Award (G.F.B.); and by institutional grant P30 DK034933 to the University of Michigan.

Abstract

Nonalcoholic fatty liver disease (NAFLD) is becoming the major chronic liver disease in many countries. Its pathogenesis is multifactorial but twin and familial studies indicate significant heritability, which is not fully explained by currently-known genetic susceptibility loci. Notably, mutations in genes encoding nuclear lamina proteins, including lamins, cause lipodystrophy syndromes that include NAFLD. We hypothesized that variants in lamina-associated proteins predispose to NAFLD and used a candidate gene-sequencing approach to test for variants in 10 nuclear lamina-related genes in a cohort of 37 twin and sibling pairs: 21 individuals with, and 53 without, NAFLD. Twelve heterozygous sequence variants were identified in four lamina-related genes (*ZMPSTE24*/*TMPO*/*SREBF1*/*SREBF2*). The majority of NAFLD patients (>90%) had at least one variant, compared to <40% of controls (P<0.0001). When only insertions/deletions and changes in conserved residues were considered, the difference between the groups was similarly striking (>80% versus <25%; P<0.0001). Presence of a lamina variant segregated with NAFLD independent of the *PNPLA3* I148M polymorphism. Several variants were found in *TMPO*, which encodes the lamina-associated polypeptide-2 (LAP2) that has not previously been associated with liver disease. One of these, a frameshift insertion that generates truncated LAP2, abrogated lamin-LAP2 binding, caused LAP2 mislocalization, altered endogenous lamin distribution, increased lipid droplet accumulation after oleic acid treatment in transfected cells, and led to cytoplasmic association with the ubiquitin-binding protein p62/SQSTM1. ***Conclusion:*** Novel variants in nuclear lamina-related genes were identified in a cohort of twins and siblings with NAFLD. One novel variant, which results in a truncated LAP2 protein and a dramatic phenotype in cell culture, represents the first association of *TMPO*/LAP2 variants with NAFLD and underscores the potential importance of the nuclear lamina in NAFLD.

Introduction

Nonalcoholic fatty liver disease (NAFLD) is now the most common form of liver disease in many countries and includes a spectrum from simple steatosis to steatohepatitis which can lead to fibrosis and ultimately cirrhosis (1-4). It is estimated that NAFLD-related cirrhosis may soon be the most common indication for liver transplant listing in the United States (5). Effective therapies for NAFLD are limited (1,6), in part due to an incomplete understanding of its pathogenesis. Twin and familial aggregation studies suggest up to 50% heritability which is not accounted for by the susceptibility loci identified to date (7-11). One possible explanation for this discrepancy is that there are genetic variants that predispose to development of NAFLD but have not yet been identified.

More than 70 human diseases have been linked to mutations in genes that encode intermediate filament proteins (IF), with no effective targeted therapy (12-14). While there are >60 cytoplasmic IF, the nuclear IF include the A- and B-type lamins which are encoded by three genes, *LMNA*/*LMNB1*/*LMNB2*. Lamins form the major components of the nuclear lamina, which is intimately associated with the inner nuclear membrane and helps maintain the nuclear structural integrity while providing a link between the cytoskeleton and the genome (15).

At least 15 disorders are caused by mutations in the genes encoding lamins (15-17). These diseases affect a number of organ systems, and in some cases the same mutation results in different phenotypes (18,19), suggesting that genetic modifiers and/or tissue-specific regulation of gene expression impact disease phenotypes. A subset of patients with germline mutations in *LMNA* develop partial lipodystrophy syndromes characterized by aberrant body fat distribution,

hyperlipidemia, insulin resistance, and hepatic steatosis (20,21). Notably, in a French cohort of 87 patients with metabolic syndrome, including many with NAFLD, three patients harbored heterozygous mutations in *LMNA* or *ZMPSTE24* (of five tested genes that encode A-type lamins or enzymes involved in lamin maturation), and >10% of the tested patients had abnormal leukocyte nuclear morphology (22,23).

Given the nearly universal liver disease in patients with lamin-related lipodystrophy and the abnormal nuclear morphology in some patients with metabolic syndrome and NAFLD (22), we hypothesized that some patients with NAFLD, but without lipodystrophy, might have variants in genes encoding lamins or lamina-related proteins that predispose to their development of NAFLD. We examined a cohort of twin and sibling pairs with NAFLD and identified several heterozygous variants in lamina-related genes, including a novel truncation variant in *TMPO*, which encodes lamina-associated polypeptide 2 (LAP2). This truncation manifests a dramatic phenotype in cell culture and is the first association of *TMPO*/LAP2 variants with NAFLD.

Materials and Methods

Study design and participants. Study participants were recruited through the NAFLD Research Center (University of California, San Diego), as part of a prospective study of twin pairs as previously reported (7,9,11) (see **Supplementary Methods**). The majority (>80%) of the cohort consisted of twin pairs, with the remainder consisting of sibling-sibling pairs; while non-twin pairs were excluded from the NAFLD heritability analysis described previously (7), they were included in this study to increase the probability of detecting rare variants. Hepatic steatosis was quantified noninvasively by magnetic resonance imaging-determined proton-density fat-fraction (MRI-PDFF), with NAFLD defined as MRI-PDFF ≥5% without apparent secondary cause of hepatic steatosis (e.g., alcohol or steatogenic medication use, other liver disease causes). Liver fibrosis was quantified by MR elastography-determined stiffness (MRE-stiffness) (7). All participants provided written informed consent, and the research protocol was approved by the Institutional Review Board. No samples were obtained from executed prisoners or other institutionalized persons.

Next-generation DNA sequencing for variant identification. Genomic DNA was isolated using the Qiagen (Redwood City, CA) DNeasy Blood and Tissue Kit. Next-generation sequencing was performed with a custom-designed TruSeq amplicon panel using a MiSeq instrument (Illumina, San Diego, CA). Variants were annotated based on RefSeq v.69 gene models and matched with 1000 Genomes Phase-3 population frequency data and dbNSFP v2.0 functional annotations (24,25)**.** Variants were confirmed by Sanger DNA sequencing using primers designed to amplify 400-600 base-pair regions of genomic DNA flanking variants of interest. The same primers were used for PCR amplification and sequencing (**Table S1**).

PNPLA3 variant genotyping. A subset of twin and sibling pairs were previously genotyped for the *PNPLA3* I148M variant (7). The remainder were genotyped using a Thermo Fisher (Waltham, MA) SNP Genotyping assay (catalog number 4351379).

Plasmids and transfection. Plasmids containing human *TMPO* (LAP2α) and *LMNA* open reading frames were purchased from Origene (Rockville, MD). The open reading frames were subcloned into pCMV6 vectors with amino-terminal green fluorescent protein (GFP) or myc/DDK tag (Origene) using *SgfI* and *MluI* restriction enzymes, with a stop codon engineered immediately 3′ to the *MluI* site. Mutants of LAP2α were generated using the QuikChange II site-directed mutagenesis kit (Agilent Technologies, Santa Clara, CA). The truncated variant of LAP2 (1-99) was generated via PCR amplification of base-pairs 1-297 of the *TMPO* open reading frame using primers engineered with flanking *SgfI* and *MluI* restriction sites, then subcloned into pCMV6 with GFP or myc/DDK tag similar to full-length LAP2α. Lipofectamine-2000 (Life Technologies, Carlsbad, CA) was used for transfection of Huh7 cells (American Type Culture Collection, Manassas, VA) (plated at ~60-70% confluency 1d prior to transfection).

Immunofluorescence. Two days after transfection, cells were washed, then fixed with a 1:1 acetone and methanol mixture (-20°C, 10min). Following fixation, washing then blocking, primary antibodies (**Table S2**) were added (overnight, 4°C). After washing, fluorescently-tagged secondary antibody (Alexa Fluor® 488 or 594; Thermo Fisher) was added (1h, 22°C), followed by DNA staining using 4',6-diamidino-2-phenylindole (DAPI) (Life Technologies). Stained cells were visualized with a Zeiss AXIO Imager.M2 microscope, and images were acquired with a 40X objective.

Fatty acid treatment. Oleic acid (Sigma-Aldrich, St. Louis, MO) stock solution (50mM) was prepared in isopropanol (26). Huh7 cells were plated on lysine-coated glass chamber slides and

transfected 1d after plating. After 2d, the culture medium was changed to DMEM containing 1% fatty acid-free BSA (Sigma-Aldrich) and oleic acid (500 μM) or vehicle. Cells were fixed (4% paraformaldehyde, 15min, 22°C) and permeabilized (0.1% Triton X-100, 5min). Blocking, antibody incubation, and DAPI mounting were performed, and 10μM BODIPY 493/503 (Thermo Fisher) was added at the primary antibody step and incubated overnight (4°C). Lipid staining was quantified by counting and measuring intracellular lipid droplets using the Zeiss Zen 2.3 lite software package (**Fig.S1**).

Semi-native and denaturing gels. Cells were solubilized in lysis buffer (1% Triton X-100, 50mM Tris pH 8.0, 150mM NaCl, protease inhibitor cocktail (Sigma-Aldrich)). After centrifugation (12,000x*g*, 10min, 4°C), the supernatant protein concentration was determined (bicinchoninic acid assay, Thermo Fisher). The supernatant was then diluted in Novex 2X Tris-glycine sample buffer with (denaturing gels) or without (semi-native gels) SDS (Invitrogen, Carlsbad, CA) with or without β-mercaptoethanol (2%). In parallel, the Triton-insoluble pellet was solubilized in SDS-containing sample buffer (95°C, 2min). Proteins were resolved using 4-20% Novex Tris-glycine native gels (Invitrogen) with running buffer containing 0.1% SDS, and visualized by silver (Thermo Fisher) or Coomassie staining.

Immunoprecipitation and immunoblotting. GFP or GFP-tagged lamin A was co-expressed in cultured cells with myc-tagged LAP2α. Two days after transfection, cells were solubilized in Triton lysis buffer (4°C, 20min), and GFP or GFP-tagged lamin A was immunoprecipitated using anti-GFP antibody and Dynabeads protein G (Invitrogen). Immunoprecipitates were resolved via SDS-PAGE and transferred to polyvinylidene fluoride membranes (Bio-Rad, Hercules, CA) for immunoblotting. Where indicated, data were quantified by densitometry using ImageJ version 1.4.3.67.

LAP2-binding protein identification by tandem mass spectrometry. Proteins were eluted by incubating the immunoprecipitates in 50µL of 0.1M glycine (pH2.5) with shaking (10min, 22°C), then addition of an equal volume of 1M Tris (pH8) prior to trypsin digestion and analysis by LC-MS/MS.

Statistical analysis. For continuous data, the two-tailed Student's *t*-test or the Mann-Whitney U test was used to assess statistical significance. For categorical data, a two-tailed Fisher's exact test was used.

Results

***Study participants*.** Thirty-seven (37) twin and sibling pairs underwent intake history, serologic evaluation, MRI, and lamina-related gene sequencing. Within this group of 74 subjects (**Table 1**), 21 met criteria for NAFLD (MRI-PDFF ≥5% without another apparent cause of hepatic steatosis). This NAFLD group consisted of five concordant twin pairs (4 monozygotic, 1 dizygotic), one concordant sibling pair, and 9 members of discordant twin (4 monozygotic, 3 dizygotic) or sibling (2) pairs. This NAFLD group was compared with 53 subjects (Controls) without NAFLD (19 concordant twin pairs, 3 concordant sibling-sibling pairs, and 9 members of discordant twin or sibling pairs). Cases and Controls differed in body mass index, hemoglobin A1c, alanine aminotransferase (ALT) levels, and MRI scores (**Table 1**). Age, sex, race, and ethnicity showed no significant differences between the two groups.

Identification of variants in lamina-related genes. Given the frequency of hepatic steatosis and steatohepatitis among patients with lipodystrophy syndromes caused by *LMNA* mutations (20,21) and the abnormal nuclear morphology in some individuals with metabolic syndrome (22), we hypothesized that variants might be found in genes encoding lamins, lamin-related proteins, or nuclear lamina-associated proteins in patients with NAFLD. To address this, we performed exon-directed sequencing of ten genes encoding lamins, lamin-binding proteins (including two transcription factors involved in lipid homeostasis that bind lamins), and lamin-processing enzymes (*LMNA*/*LMNB2*/*ZMPSTE24*/*ICMT*/*FNTA*/*FNTB*/*TMPO*/*BANF1*/*SREBF1*/*SREBF2*, **Table S3**). Sequencing was performed with an amplicon-based platform, achieving an average read coverage of 1100x across the 10 gene target with ~400 variants identified across all

samples. Of these, <10% were predicted to result in an amino acid change in the encoded protein; these were confirmed via Sanger sequencing (**Fig.S2**).

Twelve unique variants in four genes were validated (**Table 2**). Of these, *SREBF2* G595A was previously found to have a minor allele frequency (MAF) in the general population of 0.41 and, therefore, was excluded from further analyses; the remainder were novel or have MAF < 0.06 (24). Among these, novel insertion variants in *TMPO* and *SREBF2* were identified in two individuals with NAFLD. The *TMPO* insertion was also present in the monozygotic twin without NAFLD, while the *SREBF2* insertion was not present in the unaffected sibling. While no single genetic variant was significantly associated with NAFLD in this cohort after Bonferroni correction, collectively the nuclear lamina genetic variants were found preferentially in study participants with NAFLD. The majority of the patients with NAFLD (19 of 21, 90%) were heterozygous for a variant in at least one lamina-related gene, versus 19 of 53 (36%) controls (P<0.0001) (**Fig.1A,** *left panel*). When only variants predicted to result in insertion/deletion or change in a conserved amino acid were included (**Fig.1A,** *right panel*), 17 of 21 NAFLD patients (81%) carried such a variant, compared to 11 of 53 (21%) controls (P<0.0001). Similarly, the hepatic fat content (quantitated by MRI-PDFF) was compared in individuals without a lamina-related variant versus subjects with a variant (**Fig.1B**). The MRI-PDFF in the former group was 2.91±0.41% versus 6.74±0.90% in the latter group (mean±SEM;P<0.0001); when only variants predicted to result in an insertion/deletion or change in a conserved residue were included, the findings were similar: 3.02±0.34% for subjects without versus 7.93±1.12% for subjects with a variant (P<0.0001) (**Fig.1B**). Comparable results were obtained when subgroup analysis of the twin pairs (**Fig.S3**), monozygotic twin pairs (**Fig.S4A**), dizygotic twin pairs (**Fig.S4B**), and non-

twin sibling pairs (not shown) was performed separately. Similarly, when an additional 24 subjects (15 NAFLD cases, 9 controls) who were recruited as part of the same study, but not part of a twin or sibling pair, were included in the analysis, the conclusions were unchanged: 23 of 36 cases had a variant versus 24 of 62 controls (P=0.02); 20 of 36 cases had an insertion/deletion or conserved residue variant versus 14 of 62 controls (P=0.002) (**Fig.S5**).

In addition to traditional MRI, some study participants underwent MR elastography (MRE) to assess the extent of hepatic fibrosis. Within the group of 37 twin/sibling pairs (n=74 subjects), 20 of the 21 subjects with NAFLD underwent MRE. Of these, 18 of 20 (90%) had a variant in a lamina-related gene, but this high number prevented a meaningful assessment of the effect of variants on MRE-stiffness in the NAFLD group. Within the other group of 24 subjects who were not part of a twin/sibling pair (referenced above), there were 15 subjects with NAFLD, of whom 13 underwent MRE. When these 13 were combined with the 20 twins and siblings with NAFLD (n=33 total subjects with NAFLD who underwent MRE), there was a trend toward those having significant or advanced fibrosis (MRE-stiffness >3.66 kPa or >4.11 kPa, respectively (27)) being more likely to carry lamina-related variants compared to controls (P=0.2 and 0.06, respectively) (**Fig.S6**).

Effect of PNPLA3 I148M genotype. A single nucleotide polymorphism (C>G) in *PNPLA3*, which encodes patatin-like phospholipase domain containing 3, resulting in an I148M change, is a well-described susceptibility allele for NAFLD (28,29). To address whether there was any interaction between *PNPLA3* genotype and the presence of lamina-related variants in our cohort, the *PNPLA3* I148M polymorphism was genotyped in the 37 twin and sibling pairs. Notably,

presence of one or two G alleles was not significantly associated with NAFLD in our cohort (odds ratio conferred by having at least one G allele=2.48, 95% confidence interval 0.88-7.00, *P*=0.09), similar to what was previously noted (7). In contrast, the NAFLD odds ratio associated with a lamina variant was 17.0 (95% confidence interval 3.6-81.0, *P*<0.001), and the effect of a lamina variant was highest in subjects lacking a *PNPLA3* G allele (n=40): MRI-PDFF 2.40±0.17% in subjects without a lamina variant versus 5.57±0.87% in those with lamina variants (*P*<0.001) (**Fig.S7A**). Among those carrying at least one G allele (n=34), the effect of a lamina-related variant was also significant: MRI-PDFF 4.08±1.25% in those subjects without a variant versus 7.49±1.37% in those with variants (*P*=0.02). Similar findings were observed in subjects lacking a *PNPLA3* G allele when only the 31 twin pairs were examined (**Fig.S7B**), although within this subgroup the effect of a lamina variant was not as prominent among subjects carrying a *PNPLA3* G allele (*P*=0.06).

Multiple variants in TMPO. Several variants were identified in *TMPO* (**Table 2**) and were over-represented in subjects with NAFLD (13 of 21) compared to controls (10 of 53), a difference which remained significant after Bonferroni correction (*P*=0.0006 by Fisher's exact test, with a threshold of *P*<0.005 given that ten genes were tested). *TMPO* encodes six isoforms (α,β,γ,δ,ε,ζ) of lamina-associated polypeptide 2 (LAP2) that are produced via alternative splicing (**Fig.S8**). The longest isoform is known as LAP2α and was previously found to interact with lamin A/C via its carboxy terminus (30). Notably, the majority of the variants we identified in *TMPO* were in the portion of the gene that is unique to the α-isoform. The lone exception was a novel single base pair insertion (c.287_288insA) which was identified in one set of monozygotic 41 year-old twins (one twin with NAFLD and one without) and is located in the amino-terminal region

common to all isoforms. This insertion is predicted to cause a frameshift and premature stop codon after Thr 99, resulting in truncation of all LAP2 isoforms.

Two variants of LAP2 impair interaction with lamin A. The α-isoform of LAP2 is largely found in the nucleoplasm (rather than directly associated with the inner nuclear membrane) and binds and stabilizes nucleoplasmic lamin A (30-32). Previous studies have narrowed the lamin-binding domain of LAP2α to residues 601-694 (**Fig.S8**) (30). Hence, the novel truncated variant of LAP2 (LAP2 1-99) lacks the lamin-binding domain. In addition, one other variant in *TMPO* that was found in a patient with NAFLD (R690C) results in a charge change in a conserved residue and was previously reported to affect lamin binding *in vitro* (33). Interestingly, this variant was previously identified in a family with hereditary cardiomyopathy but has not been linked to liver disease (33). To address whether these variants of LAP2α affect binding to lamin A, we co-expressed GFP-tagged human lamin A with wild-type or mutant myc-tagged LAP2α in Huh7 cells and performed co-immunoprecipitation using anti-GFP antibody. GFP-tagged lamin A, but not GFP alone, readily co-precipitated wild-type LAP2α (**Fig.2A**). In agreement with a previous report showing reduced binding to the lamin A tail *in vitro* (33), LAP2α R690C exhibited a modest, though not statistically significant (quantitation via densitometry of three independent experiments – data not shown), reduction in co-precipitation with lamin A (**Fig.2A**), while a second variant of LAP2α (Q599E) located outside the lamin-binding region co-precipitated with lamin A similarly to wild-type LAP2α. In contrast, truncation of LAP2 at amino acid 99 completely abrogated binding to lamin A, despite similar expression to wild-type LAP2α (**Fig.2B**).

Full-length, but not truncated, LAP2α forms a soluble, detergent-resistant, high molecular weight species. Previous work demonstrated that the carboxy-terminal portion of LAP2α can dimerize or trimerize *in vitro* and that multimeric LAP2α migrates as a high molecular species on semi-native SDS-PAGE (34,35). Given that lamin A forms intra- and intermolecular disulfide bonds (36), we hypothesized that multimeric species of LAP2α might also be disulfide-linked. To address this, we expressed myc-tagged LAP2α in Huh7 cells, then performed SDS-PAGE under semi-native, denaturing/non-reducing, and denaturing/reducing conditions. Similar to prior findings (35), >50% of LAP2α migrated as high-molecular weight species (>250 kDa) under semi-native conditions (not shown), with identical results under denaturing non-reducing conditions (**Fig.S9A**). In contrast, under reducing conditions, >90% of LAP2α migrated as a single species (~75 kDa) consistent with monomeric LAP2α (**Fig.S9A**). These data suggest that a substantial proportion of LAP2α can exist as disulfide-linked multimeric complexes.

We hypothesized that truncated LAP2 1-99 might differ from wild-type LAP2α in its ability to form high-molecular-weight species, as the truncated protein lacks cysteines. In contrast to full-length LAP2α, LAP2 1-99 formed no disulfide-linked high-molecular-weight species (**Fig.S9A**). Notably, the LAP2α R690C variant migrated as high-molecular-weight species similar to wild-type LAP2α, consistent with a prior report (35). In addition, >50% of high-molecular-weight LAP2α species were Triton-soluble, which did not vary between wild-type LAP2α and the R690C variant. In contrast, LAP2 1-99, which did not form detectable high-molecular-weight species in the Triton-soluble fraction, formed β-mercaptoethanol-resistant insoluble high-molecular-weight forms not seen with wild-type LAP2α or any point-variant tested (**Fig.S9B**). Of note, although the high-molecular-weight smear formed by truncated LAP2 1-99 appears

more prominent after β-mercaptoethanol treatment (**Fig.S9B**), quantitation of four independent experiments showed no significant difference in the relative amount of high-molecular-weight species with or without β-mercaptoethanol treatment.

Truncation of LAP2 disrupts its nuclear localization and increases lipid accumulation compared to full-length LAP2α. In prior studies of LAP2 in cultured cells, a truncated protein containing amino acids 1-187 (generated to study LAP2 domains) lost exclusive targeting to the nucleus, suggesting that the mature protein region required for nuclear localization is C-terminal to residue 187 (37). Hence, we reasoned that LAP2 1-99 would also be mislocalized and addressed this by examining DDK-tagged full-length LAP2α or LAP2 1-99 localization in Huh7 cells. As expected, full-length LAP2α localized exclusively to the nucleus, while LAP2 1-99 was found throughout the nucleus and cytoplasm under identical conditions (**Fig.3**). Similar results were obtained in transfected human lung adenocarcinoma (A549) cells and baby hamster kidney (BHK) cells (data not shown).

To address whether LAP2 1-99 might contribute to NAFLD development by facilitating lipid accumulation in hepatocytes, we treated Huh7 cells expressing full-length LAP2α or LAP2 1-99 with oleic acid and performed lipid staining. After overnight incubation with oleic acid, lipid droplet accumulation in cells transfected with truncated LAP2 (1-99) was similar to that in adjacent untransfected cells (quantitation showed no statistically significant difference between these two groups of cells), but was significantly greater than in cells transfected with full-length LAP2α (**Fig.4**).

Truncated LAP2 has multiple unique interaction partners in Huh7 cells. Given that LAP2 1-99 exhibited unique biochemical properties compared to full-length LAP2α (**Fig.2**, **Fig.S9**), and was mislocalized in cultured cells (**Fig.3**) and led to increased lipid accumulation compared to full-length LAP2α in oleic acid-treated cells (**Fig.4**), we hypothesized that truncated LAP2 might exhibit unique protein-protein interactions compared to the full-length protein. To address this, we immunoprecipitated GFP-tagged LAP2α or LAP2 1-99 from Huh7 cell lysates and carried out mass spectrometry analysis of the immunoprecipitates and associated endogenous proteins (**Fig.5A**). Numerous unique interacting partners for truncated LAP2 1-99 as compared to full-length protein were detected, many of which were cytoplasmic proteins (**Table S4**). We selected the cytoplasmic ubiquitin-binding protein p62/SQSTM1 for validation because it ranked first among 235 identified LAP2-associated proteins after sorting by the ratio of spectra obtained with truncated LAP2 1-99 compared to full-length LAP2α, then by percent coverage, and because it was reported to regulate lipogenesis in mouse liver (38). Notably, endogenous p62/SQSTM1 interacted preferentially with LAP2 1-99 as determined by co-immunoprecipitation of GFP-tagged LAP2 followed by immunoblotting with anti-p62 antibody (**Fig.5B,C**).

Expression of truncated LAP2 alters endogenous lamin distribution in Huh7 cells. Given the unique biochemical properties of truncated LAP2 (**Fig.2**,**3**,**5**; **Fig.S9**), its effect on lipid accumulation in cells (**Fig.4**), and prior reports demonstrating a role for LAP2α in regulating lamin A/C organization (31,32), we hypothesized that LAP2 truncation might lead to altered lamin A/C organization. To address this, we expressed wild-type LAP2α and LAP2 1-99 in Huh7 cells and examined endogenous lamin A/C distribution (**Fig.6A**). Although LAP2 1-99 did not affect nuclear shape at the level of resolution we tested, more abnormal punctate and globular

lamin A/C staining was noted in nuclei of cells transfected with LAP2 1-99 as compared to full-length LAP2α (**Fig.6B**). A comparable effect was noted for B-type lamins under the same conditions (**Fig.S10**).

Discussion

Large-scale genome-wide association studies (GWAS) in individuals with NAFLD have identified several susceptibility loci (8,39), though these loci cannot account for the high degree of heritability suggested by twin and familial aggregation studies (7,8,10,11). Given that a subset of patients with mutations in *LMNA* develop lipodystrophy, metabolic syndrome, and NAFLD (20,21), as noted in mice that lack lamin A/C expression in hepatocytes (40), we reasoned that other variants in genes encoding lamin-related and lamina-associated proteins might be found in patients with NAFLD, and that rare variants that escape detection via GWAS might be identified by candidate gene sequencing approaches.

Here we report a set of variants, several of which are novel, in genes encoding lamina-related proteins in a cohort of twins and siblings with NAFLD. The majority result in a single amino acid change, while two are insertion variants (each of which was identified in one patient). Collectively these variants conferred a significantly increased risk of NAFLD within this cohort (odds ratio 17.0, $P<0.001$). In our patient cohort, the *PNPLA3* I148M polymorphism did not have a significant NAFLD effect, as noted previously (7), likely due to the small size of the cohort in relation to the frequency of this variant in the general population. Importantly, the effect of the lamina-related variants was most prominent among subjects with wild-type *PNPLA3* (CC genotype), but the interaction of lamina-related variants with *PNPLA3* genotypes will need to be assessed in a larger population.

Among the variants we identified, one set of twins with NAFLD carried a point mutation in *ZMPSTE24* (L438F), which encodes a protease involved in lamin A processing, that was

previously identified in individuals with metabolic syndrome (22,41). Notably, over one-third of the variants were in *TMPO*, most of which were located in the portion of the gene that is unique to the α-isoform of the encoded protein (LAP2). Of these, one was previously reported to cause dilated cardiomyopathy in one family (33) but has not previously been associated with metabolic disease. No disease association has previously been described for any of the other variants in *TMPO*, including the truncation at Thr99. The NAFLD patient with LAP2 1-99 has a monozygotic twin with normal MRI-PDFF, underlining the importance of environmental factors in NAFLD and suggesting that this truncation may represent a predisposition rather than a high-penetrance cause of NAFLD. However, the possibility of other NAFLD patients carrying *TMPO* variants will need to be investigated, and it is not possible to make definitive genotype-phenotype conclusions because of the small numbers and the lack of longitudinal and clinical/lifestyle information, as the involved twins were lost to follow-up after their initial enrollment in 2012 (**Table S5**).

The dramatic effects of truncated LAP2 1-99 in transfected cells, including its altered intracellular distribution, alteration of endogenous lamin distribution, and increased lipid droplet accumulation, support a role for this variant in predisposition to liver disease. Truncated LAP2 robustly co-precipitated endogenous p62/SQSTM1, which regulates lipogenic gene expression in mouse liver (38), but the functional importance of this and the other unique protein-protein interactions identified via mass spectrometry remain to be defined. In addition, the effects of truncated LAP2 on both A- and B-type lamins (**Fig.6**, **Fig.S10**) are noteworthy given previous studies showing that *Lmnb1* and *Lmnb2* depletion in hepatocytes did not lead to misshapen nuclei as determined by liver tissue staining but did lead to nuclear blebbing of cultured

hepatocytes (42). It is unknown whether these mice develop spontaneous hepatosteatosis upon aging or have increased susceptibility to fibrosis upon high fat feeding as was noted in hepatocyte-specific *Lmna*-null mice (40). However, liver involvement was reported in a patient with acquired partial lipodystrophy due to *LMNB2* mutation (23,43). In addition, alterations of lamins A/C and B1/B2 occur in the context Mallory-Denk body formation and porphyria-associated liver injury (44,45).

Limitations of our findings include the relatively small number of participants which precludes statistical significance for any individual variant. Nevertheless, the fact that we identified several variants, even in our small cohort, underscores the potential importance of the nuclear lamina in NAFLD and the need for further study. Another limitation is that non-invasive assessment of liver disease was used rather than liver biopsy. While the accuracy of MRI in assessing hepatic steatosis is well-established (46), the lack of histologic data precludes definitive conclusions about liver disease severity. Still, among study participants who underwent MRE, there was a trend toward higher MRE-stiffness among those subjects carrying lamina-related variants (**Fig.S6**). This suggests the possibility that these variants might contribute to liver disease progression but such a conclusion requires study in larger cohorts.

The data presented here have a number of implications for the study of nuclear lamina function, lamina-related disease, and NAFLD. Our findings underscore the importance of proper localization and interaction of lamins and lamin-binding proteins at the nuclear lamina. Prior studies in cell culture systems and mice have illustrated the role of LAP2α-lamin interaction in regulating the stability, localization, and function of lamin A/C (31,32). Our findings are the first

to suggest a potential link of *TMPO* variants with liver disease, possibly via impaired interaction with lamin A. In this context, one of the *TMPO* variants identified herein, the R690C variant, was previously reported to cause dilated cardiomyopathy (33), or to serve as a genetic modifier in a family with dilated cardiomyopathy (47), without the description of liver disease. Identification of this variant in an individual with NAFLD underscores the variability in laminopathy phenotypes and the likelihood that genetic modifiers influence both the severity of disease and the affected organ(s). In addition, extrapolation of the number of patients in our small cohort with variants (19 of 21) in the ten genes sequenced raises the possibility that they might be relatively common among patients with familial NAFLD. We also posit that some patients with nonfamilial NAFLD might have an unrecognized laminopathy, which may have future therapeutic implications as drugs are developed to target laminopathies (48). Further study in larger patient cohorts will be needed to clarify the frequency and relative contributions of variants in lamina-related genes in patients with NAFLD. Taken together, our data suggest several mechanisms by which lamina-related variants such as truncated LAP2 1-99 might promote susceptibility to NAFLD via inappropriate interaction with cytoplasmic proteins including p62/SQSTM1, altered lamin distribution (which could alter chromatin organization (49) and cause downstream transcriptional changes (50)), and promotion of lipid accumulation in hepatocytes (**Fig.6C**).

Acknowledgements: The authors would like to thank Dr. Robert Lyons and Jeanne Geskes of the University of Michigan DNA Sequencing core for their assistance with next-generation DNA

sequencing, and members of the Omary laboratory for helpful discussions and critical review of the manuscript.

References

1. Chalasani N, Younossi Z, Lavine JE, Diehl AM, Brunt EM, Cusi K, et al. The diagnosis and management of non-alcoholic fatty liver disease: practice Guideline by the American Association for the Study of Liver Diseases, American College of Gastroenterology, and the American Gastroenterological Association. Hepatology 2012;55:2005-2023.

2. Michelotti GA, Machado MV, Diehl AM. NAFLD, NASH and liver cancer. Nat Rev Gastroenterol Hepatol 2013;10:656-665.

3. Sattar N, Forrest E, Preiss D. Non-alcoholic fatty liver disease. BMJ 2014;349:g4596.

4. Marengo A, Jouness RI, Bugianesi E. Progression and Natural History of Nonalcoholic Fatty Liver Disease in Adults. Clin Liver Dis 2016;20:313-324.

5. Wong RJ, Aguilar M, Cheung R, Perumpail RB, Harrison SA, Younossi ZM, Ahmed A. Nonalcoholic steatohepatitis is the second leading etiology of liver disease among adults awaiting liver transplantation in the United States. Gastroenterology 2015;148:547-555.

6. Sanyal AJ, Chalasani N, Kowdley KV, McCullough A, Diehl AM, Bass NM, et al. Pioglitazone, vitamin E, or placebo for nonalcoholic steatohepatitis. N Engl J Med 2010;362:1675-1685.

7. Loomba R, Schork N, Chen CH, Bettencourt R, Bhatt A, Ang B, et al. Heritability of Hepatic Fibrosis and Steatosis Based on a Prospective Twin Study. Gastroenterology 2015;149:1784-1793.

8. Anstee QM, Seth D, Day CP. Genetic Factors That Affect Risk of Alcoholic and Nonalcoholic Fatty Liver Disease. Gastroenterology 2016;150:1728-1744 e1727.

9. Zarrinpar A, Gupta S, Maurya MR, Subramaniam S, Loomba R. Serum microRNAs explain discordance of non-alcoholic fatty liver disease in monozygotic and dizygotic twins: a prospective study. Gut 2016;65:1546-1554.

10. Grove JI, Austin M, Tibble J, Aithal GP, Verma S. Monozygotic twins with NASH cirrhosis: cumulative effect of multiple single nucleotide polymorphisms? Ann Hepatol 2016;15:277-282.

11. Cui J, Chen CH, Lo MT, Schork N, Bettencourt R, Gonzalez MP, et al. Shared genetic effects between hepatic steatosis and fibrosis: A prospective twin study. Hepatology 2016;64:1547-1558.

12. Omary MB. "IF-pathies": a broad spectrum of intermediate filament-associated diseases. J Clin Invest 2009;119:1756-1762.

13. Butin-Israeli V, Adam SA, Goldman AE, Goldman RD. Nuclear lamin functions and disease. Trends Genet 2012;28:464-471.

14. Sun J, Groppi VE, Gui H, Chen L, Xie Q, Liu L, Omary MB. High-Throughput Screening for Drugs that Modulate Intermediate Filament Proteins. Methods Enzymol 2016;568:163-185.

15. Burke B, Stewart CL. The nuclear lamins: flexibility in function. Nat Rev Mol Cell Biol 2013;14:13-24.

16. Worman HJ, Fong LG, Muchir A, Young SG. Laminopathies and the long strange trip from basic cell biology to therapy. J Clin Invest 2009;119:1825-1836.

17. Davidson PM, Lammerding J. Broken nuclei--lamins, nuclear mechanics, and disease. Trends Cell Biol 2014;24:247-256.

18. Taylor MR, Fain PR, Sinagra G, Robinson ML, Robertson AD, Carniel E, et al. Natural history of dilated cardiomyopathy due to lamin A/C gene mutations. J Am Coll Cardiol 2003;41:771-780.

19. **Van Esch H, Agarwal AK**, Debeer P, Fryns JP, Garg A. A homozygous mutation in the lamin A/C gene associated with a novel syndrome of arthropathy, tendinous calcinosis, and progeroid features. J Clin Endocrinol Metab 2006;91:517-521.

20. Guenantin AC, Briand N, Bidault G, Afonso P, Bereziat V, Vatier C, et al. Nuclear envelope-related lipodystrophies. Semin Cell Dev Biol 2014;29:148-157.

21. Ajluni N, Meral R, Neidert AH, Brady GF, Buras E, McKenna B, et al. Spectrum of disease associated with partial lipodystrophy: lessons from a trial cohort. Clin Endocrinol (Oxf) 2017;86:698-707.

22. **Dutour A, Roll P**, Gaborit B, Courrier S, Alessi MC, Tregouet DA, et al. High prevalence of laminopathies among patients with metabolic syndrome. Hum Mol Genet 2011;20:3779-3786.

23. Omary MB. Intermediate filament proteins of digestive organs: physiology and pathophysiology. Am J Physiol Gastrointest Liver Physiol 2017;312:G628-G634.

24. 1000 Genomes Project Consortium (Auton A, Brooks LD, Durbin RM, Garrison EP, Kang HM, Korbel JO, et al.). A global reference for human genetic variation. Nature 2015;526:68-74.

25. Liu X, Jian X, Boerwinkle E. dbNSFP v2.0: a database of human non-synonymous SNVs and their functional predictions and annotations. Hum Mutat 2013;34:E2393-2402.

26. Malhi H, Bronk SF, Werneburg NW, Gores GJ. Free fatty acids induce JNK-dependent hepatocyte lipoapoptosis. J Biol Chem 2006;281:12093-12101.

27. Singh S, Venkatesh SK, Wang Z, Miller FH, Motosugi U, Low RN, et al. Diagnostic performance of magnetic resonance elastography in staging liver fibrosis: a systematic review and meta-analysis of individual participant data. Clin Gastroenterol Hepatol 2015;13:440-451 e446.

28. **Romeo S, Kozlitina J**, Xing C, Pertsemlidis A, Cox D, Pennacchio LA, et al. Genetic variation in PNPLA3 confers susceptibility to nonalcoholic fatty liver disease. Nat Genet 2008;40:1461-1465.

29. Speliotes EK, Butler JL, Palmer CD, Voight BF, GIANT Consortium, MIGen Consortium, et al. PNPLA3 variants specifically confer increased risk for histologic nonalcoholic fatty liver disease but not metabolic disease. Hepatology 2010;52:904-912.

30. Dechat T, Korbei B, Vaughan OA, Vlcek S, Hutchison CJ, Foisner R. Lamina-associated polypeptide 2alpha binds intranuclear A-type lamins. J Cell Sci 2000;113 Pt 19:3473-3484.

31. **Naetar N, Korbei B**, Kozlov S, Kerenyi MA, Dorner D, Kral R, et al. Loss of nucleoplasmic LAP2alpha-lamin A complexes causes erythroid and epidermal progenitor hyperproliferation. Nat Cell Biol 2008;10:1341-1348.

32. Gesson K, Vidak S, Foisner R. Lamina-associated polypeptide (LAP)2alpha and nucleoplasmic lamins in adult stem cell regulation and disease. Semin Cell Dev Biol 2014;29:116-124.

33. Taylor MR, Slavov D, Gajewski A, Vlcek S, Ku L, Fain PR, et al. Thymopoietin (lamina-associated polypeptide 2) gene mutation associated with dilated cardiomyopathy. Hum Mutat 2005;26:566-574.

34. **Bradley CM, Jones S**, Huang Y, Suzuki Y, Kvaratskhelia M, Hickman AB, et al. Structural basis for dimerization of LAP2alpha, a component of the nuclear lamina. Structure 2007;15:643-653.

35. Snyers L, Vlcek S, Dechat T, Skegro D, Korbei B, Gajewski A, et al. Lamina-associated polypeptide 2-alpha forms homo-trimers via its C terminus, and oligomerization is unaffected by a disease-causing mutation. J Biol Chem 2007;282:6308-6315.

36. **Pekovic V, Gibbs-Seymour I**, Markiewicz E, Alzoghaibi F, Benham AM, Edwards R, et al. Conserved cysteine residues in the mammalian lamin A tail are essential for cellular responses to ROS generation. Aging Cell 2011;10:1067-1079.

37. Vlcek S, Just H, Dechat T, Foisner R. Functional diversity of LAP2alpha and LAP2beta in postmitotic chromosome association is caused by an alpha-specific nuclear targeting domain. EMBO J 1999;18:6370-6384.

38. Popineau L, Morzyglod L, Carre N, Cauzac M, Bossard P, Prip-Buus C, et al. Novel Grb14-Mediated Cross Talk between Insulin and p62/Nrf2 Pathways Regulates Liver Lipogenesis and Selective Insulin Resistance. Mol Cell Biol 2016;36:2168-2181.

39. **Speliotes EK, Yerges-Armstrong LM, Wu J, Hernaez R, Kim LJ**, Palmer CD, et al. Genome-wide association analysis identifies variants associated with nonalcoholic fatty liver disease that have distinct effects on metabolic traits. PLoS Genet 2011;7:e1001324.

40. Kwan R, Brady GF, Brzozowski M, Weerasinghe SV, Martin H, Park M-J, et al. Hepatocyte-specific deletion of mouse lamin A/C leads to male-selective steatohepatitis. Cell Mol Gastroenterol Hepatol 2017 (*in press*).

41. Galant D, Gaborit B, Desgrouas C, Abdesselam I, Bernard M, Levy N, et al. A Heterozygous ZMPSTE24 Mutation Associated with Severe Metabolic Syndrome, Ectopic Fat Accumulation, and Dilated Cardiomyopathy. Cells 2016;5.

42. Yang SH, Jung HJ, Coffinier C, Fong LG, Young SG. Are B-type lamins essential in all mammalian cells? Nucleus 2011;2:562-569.

43. Gao J, Li Y, Fu X, Luo X. A Chinese patient with acquired partial lipodystrophy caused by a novel mutation with LMNB2 gene. J Pediatr Endocrinol Metab 2012;25:375-377.

44. Zatloukal K, Denk H, Spurej G, Hutter H. Modulation of protein composition of nuclear lamina. Reduction of lamins B1 and B2 in livers of griseofulvin-treated mice. Lab Invest 1992;66:589-597.

45. Singla A, Griggs NW, Kwan R, Snider NT, Maitra D, Ernst SA, et al. Lamin aggregation is an early sensor of porphyria-induced liver injury. J Cell Sci 2013;126:3105-3112.

46. Reeder SB, Sirlin CB. Quantification of liver fat with magnetic resonance imaging. Magn Reson Imaging Clin N Am 2010;18:337-357.

47. Zaragoza MV, Fung L, Jensen E, Oh F, Cung K, McCarthy LA, et al. Exome Sequencing Identifies a Novel LMNA Splice-Site Mutation and Multigenic Heterozygosity of Potential Modifiers in a Family with Sick Sinus Syndrome, Dilated Cardiomyopathy, and Sudden Cardiac Death. PLoS One 2016;11:e0155421.

48. Muchir A, Worman HJ. Targeting Mitogen-Activated Protein Kinase Signaling in Mouse Models of Cardiomyopathy Caused by Lamin A/C Gene Mutations. Methods Enzymol 2016;568:557-580.

49. Barton LJ, Soshnev AA, Geyer PK. Networking in the nucleus: a spotlight on LEM-domain proteins. Curr Opin Cell Biol 2015;34:1-8.

50. Vidak S, Kubben N, Dechat T, Foisner R. Proliferation of progeria cells is enhanced by lamina-associated polypeptide 2alpha (LAP2alpha) through expression of extracellular matrix proteins. Genes Dev 2015;29:2022-2036.

Author names in bold designate co-first authorship.

Parameter	Cases (n = 21) [with NAFLD]	Controls (n = 53) [without NAFLD]	*P*-value
Age (S.D.)	52.1 (19.6)	46.1 (20.6)	0.26
% Male	57	32	0.07
% Caucasian	67	51	0.30
% Hispanic	24	15	0.27
BMI (S.D.)	32.3 (5.0)	27.2 (5.4)	< 0.001
Hgb A1c (S.D.)	6.1 (0.7)	5.7 (0.4)	0.001
ALT (S.D.)	30 (18)	21 (12)	0.01
MRI-PDFF (S.D.)	10.7 (5.4)	2.6 (0.9)	< 0.0001

Table 1. Characteristics of twin and sibling cohort (37 pairs, n=74 subjects). S.D., standard deviation; BMI, body mass index; Hgb, hemoglobin.

Gene	Nucleotide change	Amino acid change	Conserved residue	Number of cases with variant	Number of controls with variant	Minor allele frequency
ZMPSTE24	C > T	L438F	Yes	2	0	0.001
TMPO	InsA	T99fs	N/A	1	1	Not identified
TMPO	G > A	R274K	No	0	1	0.002
TMPO	C > G	T317S	Yes	0	1	0.030
TMPO	C > G	Q599E	Yes	11	7	0.06
TMPO	C > T	R690C	Yes	1	0	0.011
SREBF1	C > T	V610M	Yes	1	1	0.007
SREBF2	Ins (24bp)	S72Ins (in-frame)	N/A	1	0	Not identified
SREBF2	G > A	R371K	Yes	0	2	0.001
SREBF2	G > C	G595A	No	16	23	0.41
SREBF2	G > C	R860S	No	6	7	0.06
SREBF2	G > A	R1080Q	Yes	1	0	0.001

Table 2. Confirmed coding variants. Minor allele frequency (MAF) cited in far right column is derived from the 1000 Genomes Project (reference 24). Ins, insertion; fs, frameshift.

Figure Legends - HEP-17-0541.R2

Figure 1. Variants in lamina-related genes were predominantly found in individuals with NAFLD in a cohort of twin and sibling pairs. (A) *Left panel*: Percentages of individuals (*y*-axis) with and without genetic variants are shown for both NAFLD cases and Controls (includes all coding variants with minor allele frequency < 0.06). *Right panel:* Percentages of individuals (*y*-axis) with and without a variant resulting in insertion/deletion or change in a conserved residue are shown for NAFLD cases and Controls. Fisher's exact test was used to assess statistical significance at a threshold of $P<0.05$. (B) *Left panel*: Scatter plot of liver fat content (assessed by MRI-PDFF) of individuals without and with a lamina-related genetic variant (includes all coding variants with minor allele frequency < 0.06). *Right panel*: Scatter plot of liver fat content (assessed by MRI-PDFF) of individuals without and with a lamina-related genetic variant (includes variants resulting in insertion/deletion or change in a conserved residue). Error bars represent standard error of the mean. Mann-Whitney U test was used to assess statistical significance at a threshold of $P<0.05$.

Figure 2. Variants of LAP2 found in NAFLD patients interfere with binding to lamin A. (A) Huh7 cells were co-transfected with myc-tagged wild-type (WT) or variant LAP2α and GFP-tagged lamin A, followed by immunoprecipitation using an antibody directed to the GFP tag. Immunoprecipitates were resolved on SDS-PAGE, and precipitated proteins were visualized after immunoblotting with antibodies to myc or the GFP tag. (B) Huh7 cells were co-transfected with GFP-tagged lamin A and WT LAP2α or its truncated variant (LAP2 1-99). Lamin A was immunoprecipitated, followed by visualization as in panel A. Ig, immunoglobulin; M.W.,

apparent molecular weight; kDa, kilodaltons; IP, immunoprecipitation; IB, immunoblot. Arrowhead indicates a non-specific band recognized by the myc antibody.

Figure 3. The truncated variant of LAP2 is mislocalized in transfected cells. (A) Huh7 cells were transfected with full-length (F.L.) LAP2α or truncated LAP2 (1-99) with DDK tag, or empty vector. Cells were then fixed, and LAP2 was visualized by indirect immunofluorescence using anti-FLAG antibody (which recognizes the DDK tag). Scale bar: 50 μm (lower magnification images: first, second, and fourth rows), 20 μm (higher magnification images: third and fifth rows). (B) Cells transfected as in panel A were scored according to whether LAP2 was specifically localized to the nucleus or mislocalized throughout the cell (represented as percent of transfected cells with mislocalized LAP2). Data were derived from counting 9-12 high-power fields from three independent experiments. Error bars represent the standard error of the mean. Student's *t* test was used to determine statistical significance at a threshold of $P<0.05$.

Figure 4. Truncated LAP2 causes increased lipid accumulation in transfected cells. (A) Huh7 cells were transfected with DDK-tagged full-length (F.L.) LAP2α or truncated LAP2 (1-99) or empty vector, then treated with 500 μM oleic acid or vehicle (isopropanol) in serum-free medium overnight. After fixation, transfected LAP2 was visualized by indirect immunofluorescence using anti-FLAG antibody. Lipid droplets were stained with BODIPY 493/593 as described in Materials and Methods. Representative images are shown for each condition; scale bar, 20 μm. (B) Lipid accumulation was quantitated as described in Materials and Methods for >10 high-power fields for each condition, and the data shown are representative

of 3 independent experiments. Error bars represent standard error of the mean. Student's *t* test was used to determine statistical significance at a threshold of $P<0.05$.

Figure 5. Truncated LAP2 has multiple unique cytoplasmic interaction partners, including p62/SQSTM1. (A) Huh7 cells were transfected with GFP-tagged LAP2α or truncated LAP2 (1-99), followed by immunoprecipitation using an anti-GFP antibody; empty vector (GFP only) and GFP-tagged lamin A were included as controls. The immunoprecipitates and the input cell lysates were visualized by silver staining. (B) Huh7 cells were transfected with GFP alone, GFP-tagged LAP2α, or truncated LAP2 (1-99), followed by immunoprecipitation of LAP2 using anti-GFP antibody. Co-precipitated p62/SQSTM1 was visualized by immunoblotting. (C) Immunoprecipitated GFP and GFP-tagged proteins were visualized by Coomassie staining for the samples shown in panel B. M.W., apparent molecular weight; kDa, kilodaltons; IP, immunoprecipitates. Arrowheads indicate antibody heavy (~50 kDa) and light (~25 kDa) chains.

Figure 6. Truncated LAP2 causes altered lamin A/C distribution. (A) Huh7 cells were transfected with DDK-tagged full-length (F.L.) LAP2α or truncated LAP2 (1-99). After fixation, transfected LAP2 and endogenous lamin A/C were visualized by immunofluorescence using anti-FLAG and anti-lamin A/C antibodies, respectively. Representative high-magnification images are shown; nuclei of transfected cells with abnormal lamin A/C staining (punctate/globular) are highlighted by arrows. Scale bar, 20 μm. (B) Nuclear morphology and lamin A/C distribution in cells transfected with full-length LAP2α or truncated LAP2 (1-99) were scored in a blinded fashion from three independent experiments (3-6 fields/condition/experiment, >85 total nuclei/condition). Error bars represent standard error of

the mean. Student's *t* test was used to determine statistical significance; ***, $P<0.001$. (C) Schematic of alterations predicted to occur due to expression of LAP2 1-99, thereby predisposing to NAFLD via ectopic protein-protein interactions (e.g., LAP2 1-99 with p62/SQSTM1), altered lamin A/C distribution, chromatin reorganization, and increased lipid accumulation in hepatocytes. ONM, outer nuclear membrane; INM, inner nuclear membrane.

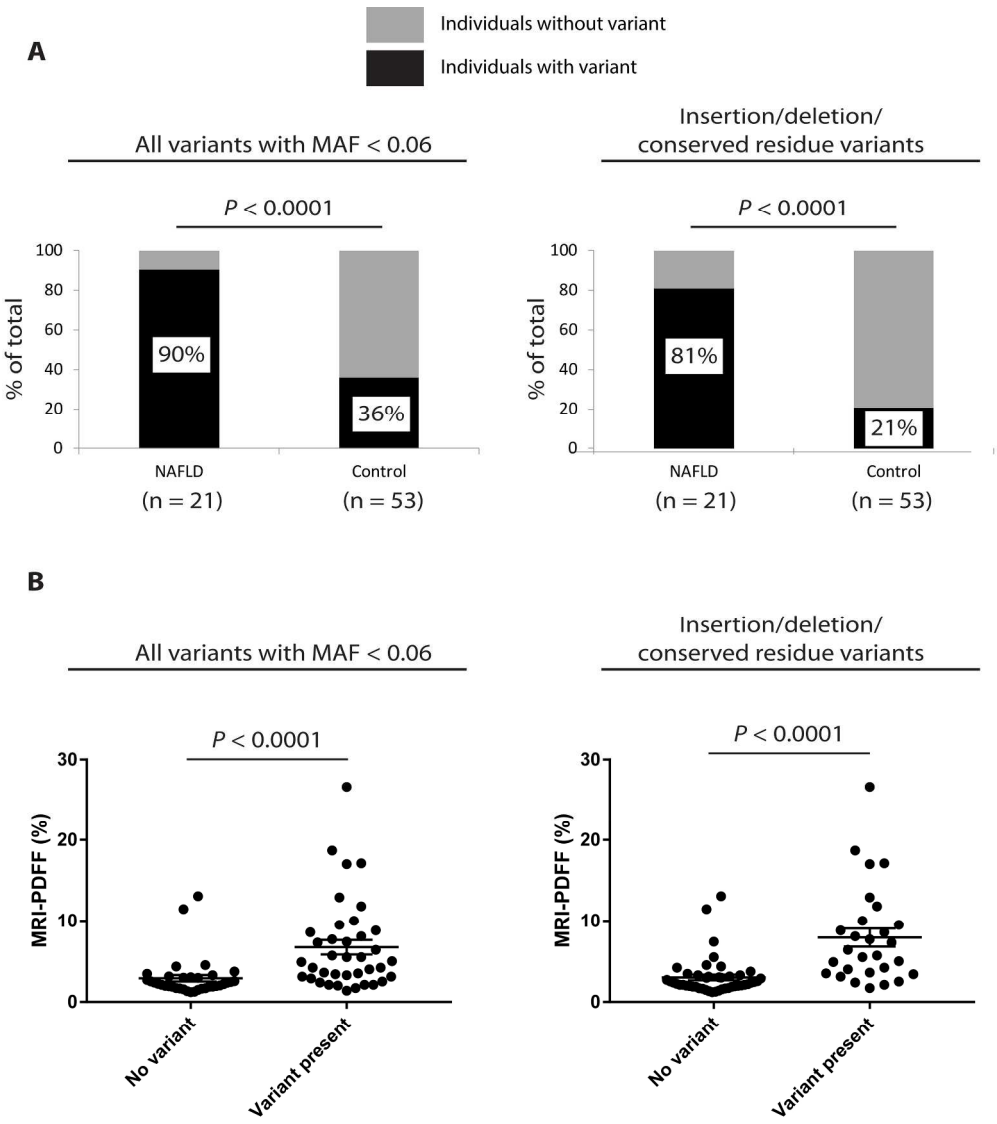

Figure 1

234x261mm (300 x 300 DPI)

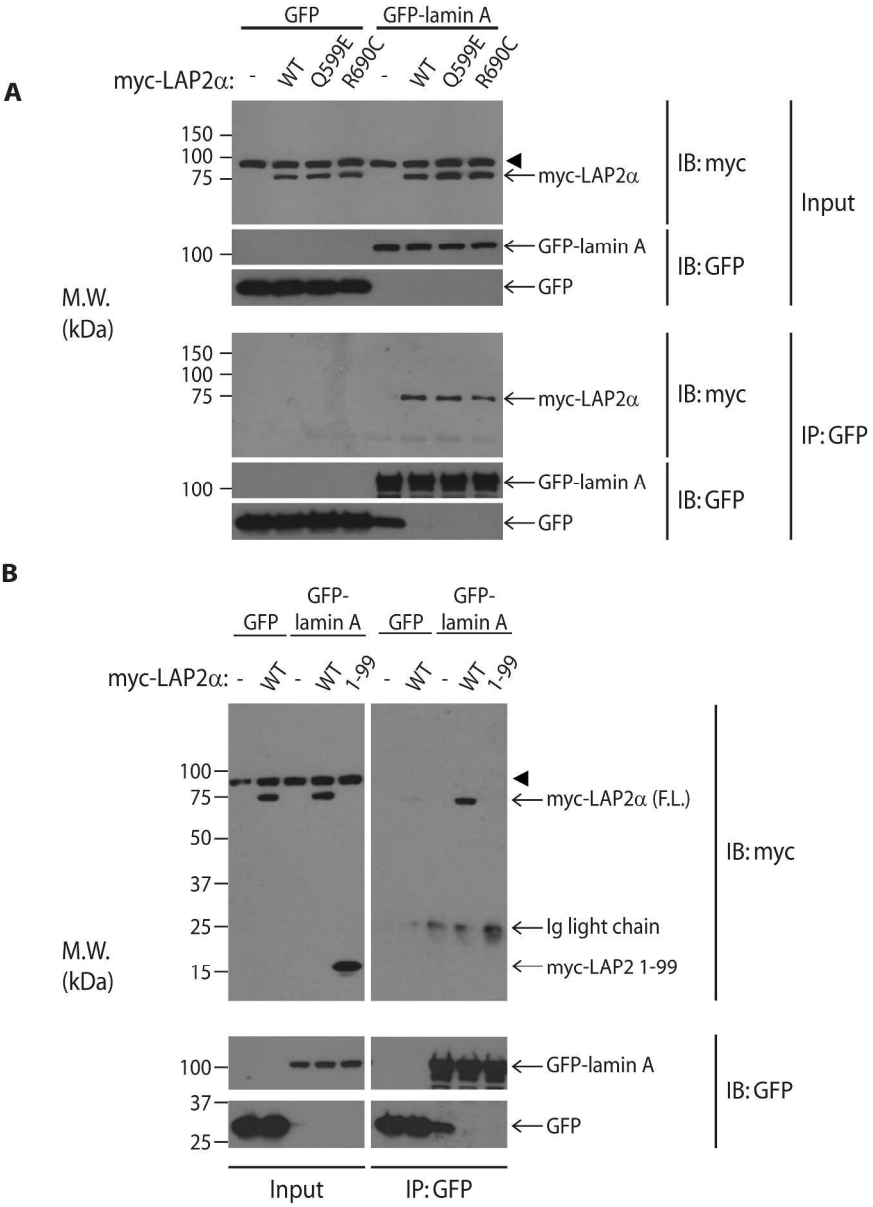

Figure 2

259x359mm (300 x 300 DPI)

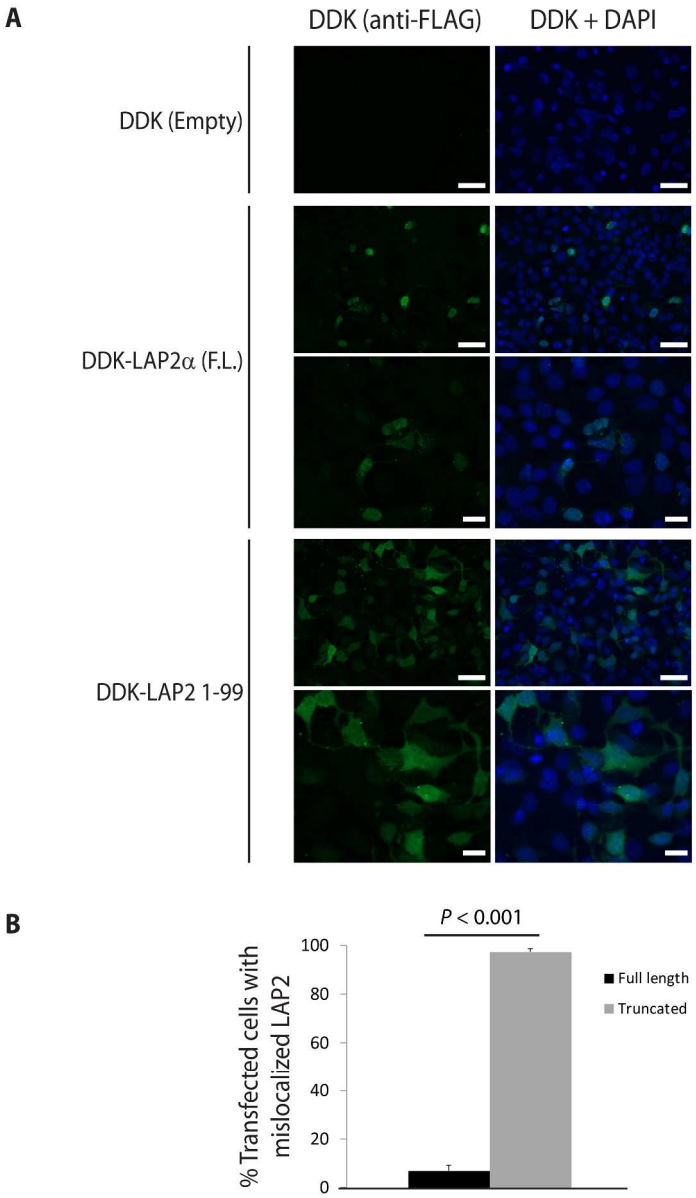

Figure 3

269x435mm (300 x 300 DPI)

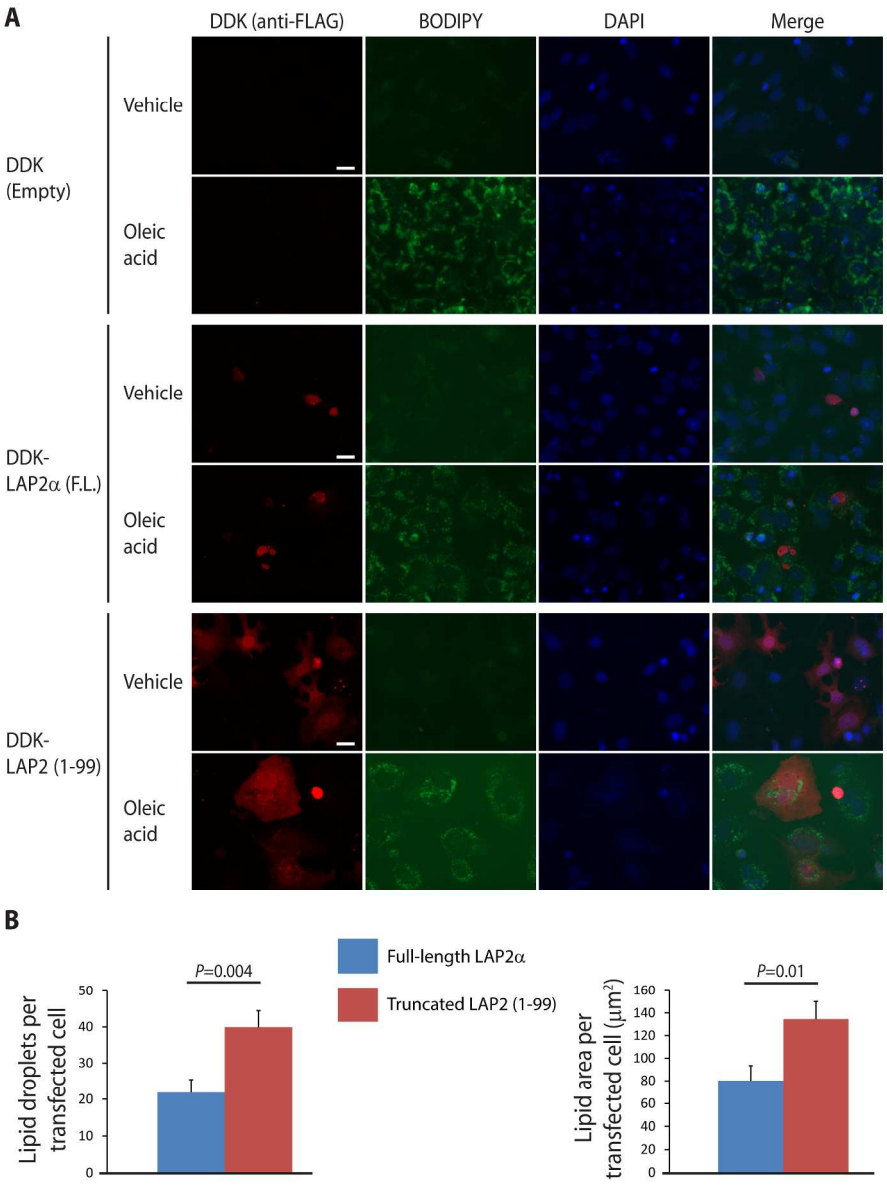

Figure 4

270x319mm (300 x 300 DPI)

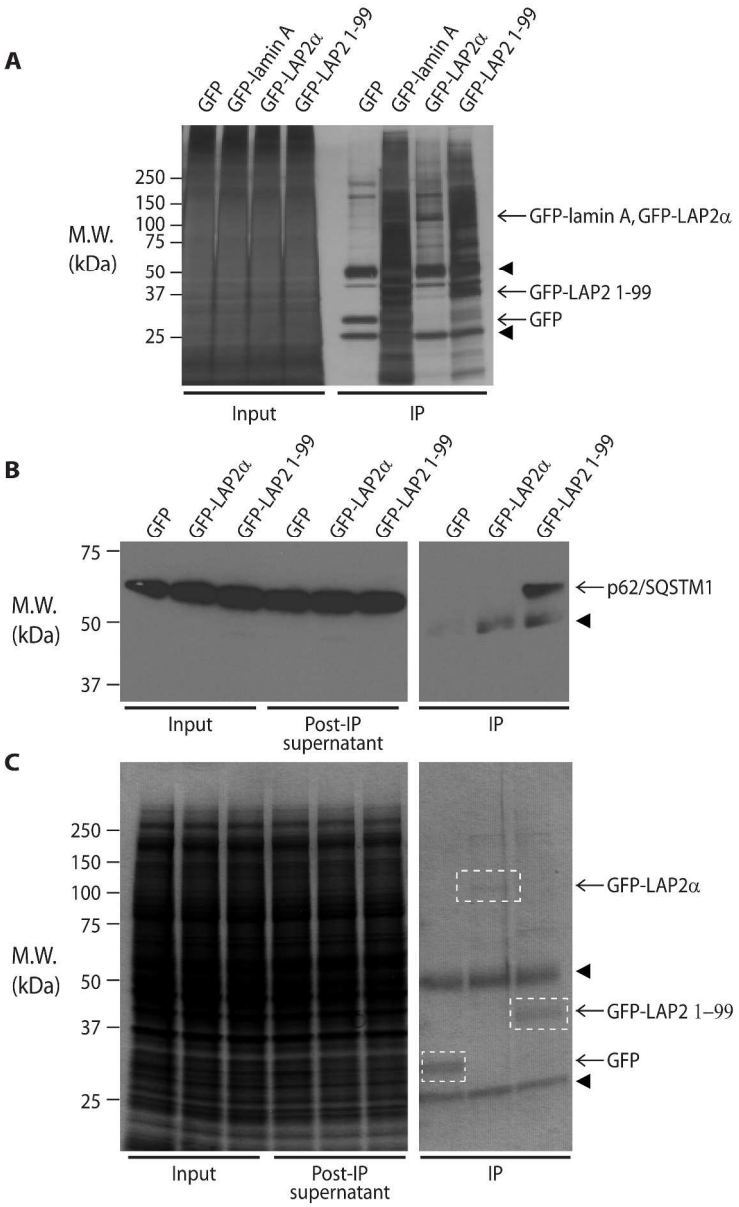

Figure 5

276x455mm (300 x 300 DPI)

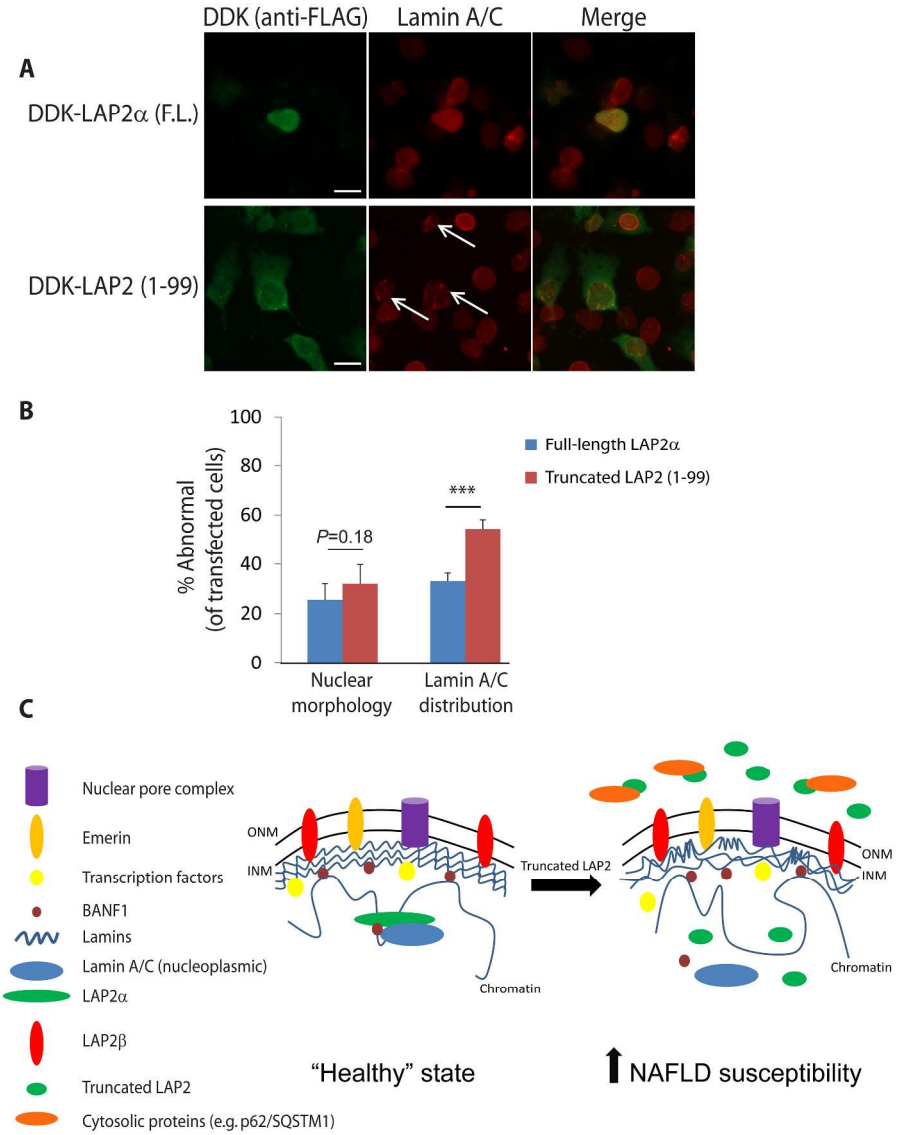

Figure 6

282x347mm (300 x 300 DPI)

Fig S1

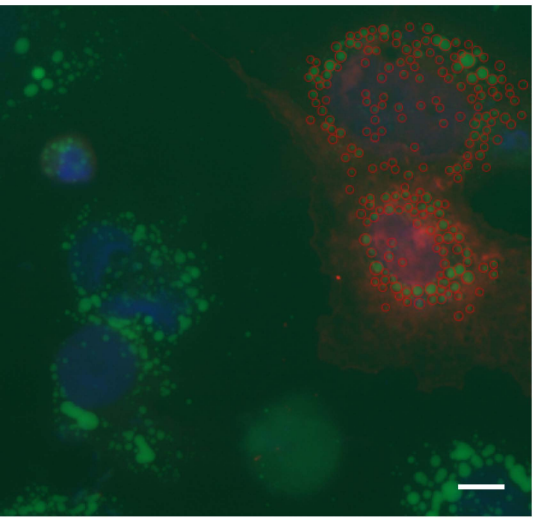

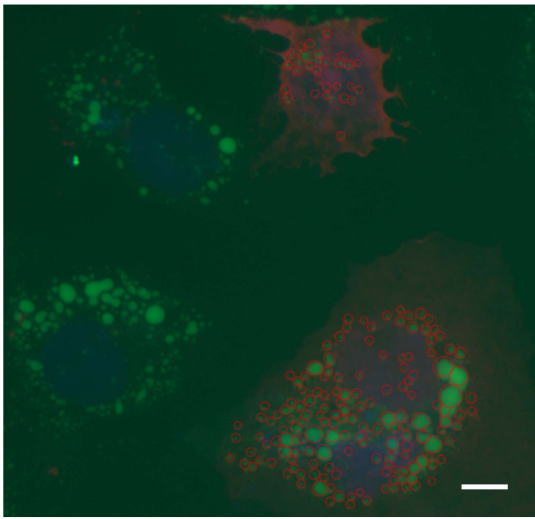

Fig. S1. Quantitation of lipid droplets in oleic acid-treated Huh7 cells. Lipid droplets were stained with BODIPY 493/503 and imaged as described in Materials and Methods. Lipid droplet accumulation was quantitated by drawing a circle around each droplet using the Zeiss Zen 2.3 lite software package to measure the diameter and area. Two such images with circled lipid droplets are shown. Scale bar, 10 μm.

Fig S2

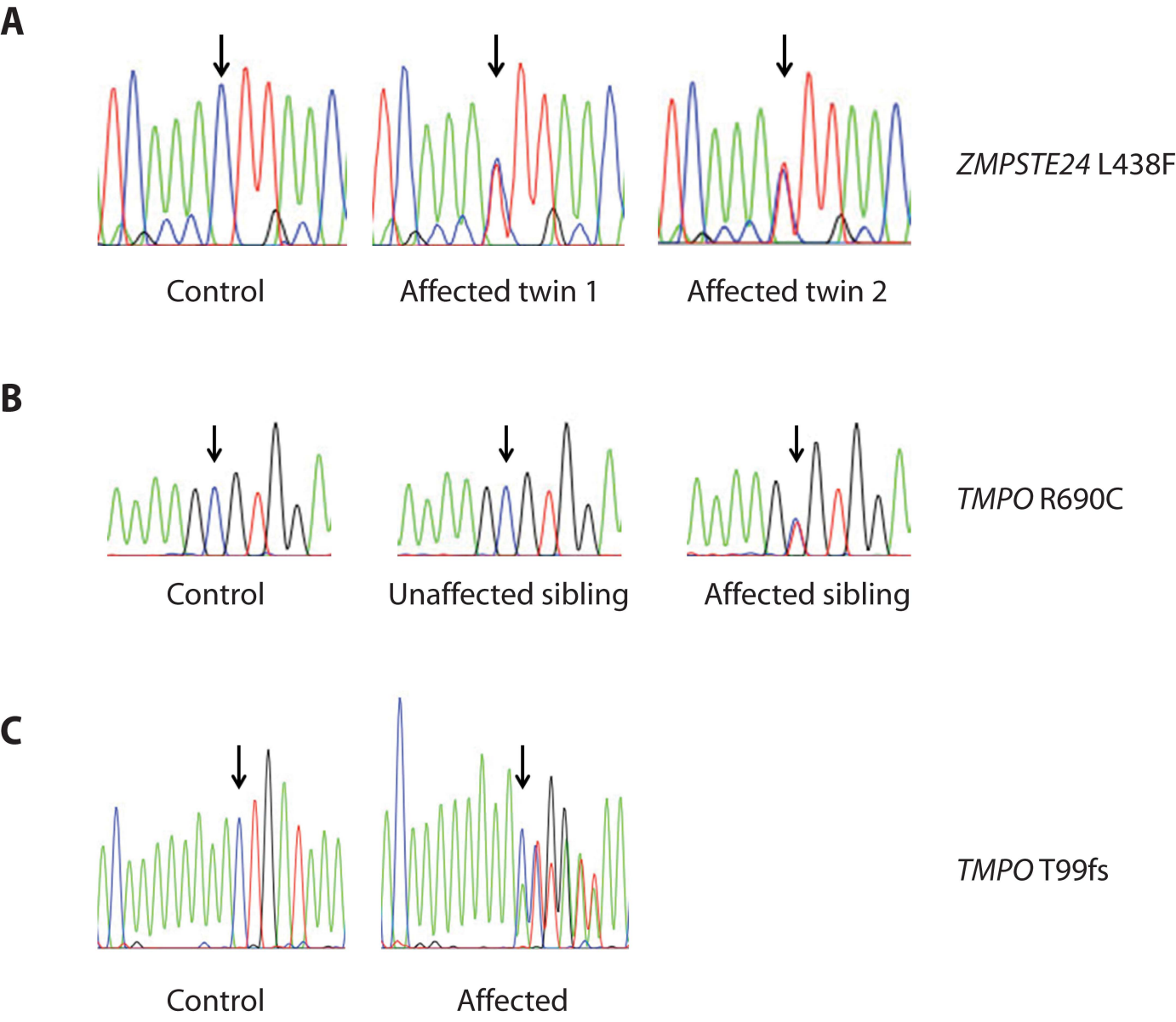

Fig. S2. Selected chromatograms showing confirmation of lamina-related variants in individuals with NAFLD. (A) Two twins with NAFLD carrying the L438F variant in the gene encoding the ZMPSTE24 protease, which cleaves lamin A (C > T change in genomic DNA). (B) NAFLD patient with C > T change in *TMPO* (which encodes the six isoforms of LAP2), resulting in the LAP2α R690C variant. An unrelated control and the patient's unaffected sibling are shown for comparison. (C) NAFLD patient with single base-pair insertion in *TMPO* resulting in a frameshift (fs) and premature stop codon after Thr 99 in the LAP2 protein. Arrows indicate the changed nucleotide in each case; all variants were confirmed by Sanger sequencing of both sense and antisense strands.

Fig S3

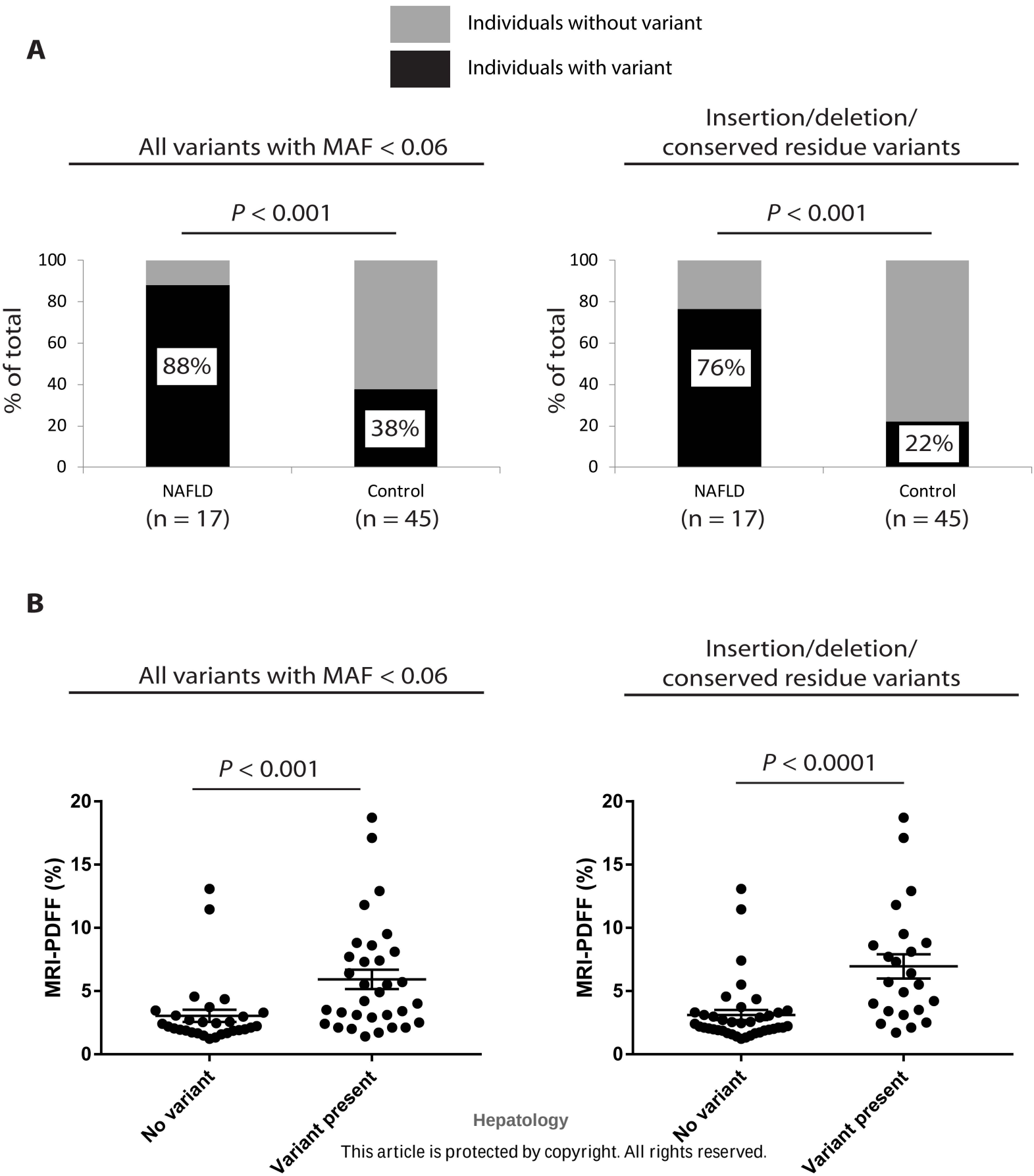

Fig. S3. Among twin pairs only (31 pairs, n=62 subjects), variants in lamina-related genes were predominantly found in twins with NAFLD. (A) *Left panel*: Percentages of twins (*y*-axis) with and without genetic variants are shown for NAFLD cases and Controls (includes all coding variants with minor allele frequency < 0.06). *Right panel:* Percentages of twins (*y*-axis) with and without a variant resulting in insertion/deletion or change in a conserved residue are shown for NAFLD cases and Controls. Fisher's exact test was used to assess statistical significance at a threshold of $P<0.05$. (B) *Left panel*: Scatter plot of liver fat content (assessed by MRI-PDFF) of twins (31 pairs, n=62 subjects) without and with a lamina-related genetic variant (includes all coding variants with minor allele frequency < 0.06). *Right panel*: Scatter plot of liver fat content (assessed by MRI-PDFF) of twins without and with a lamina-related genetic variant (includes variants resulting in insertion/deletion or change in a conserved residue). Error bars represent standard error of the mean; Mann-Whitney U test was used to assess statistical significance at a threshold of $P<0.05$.

Fig S4

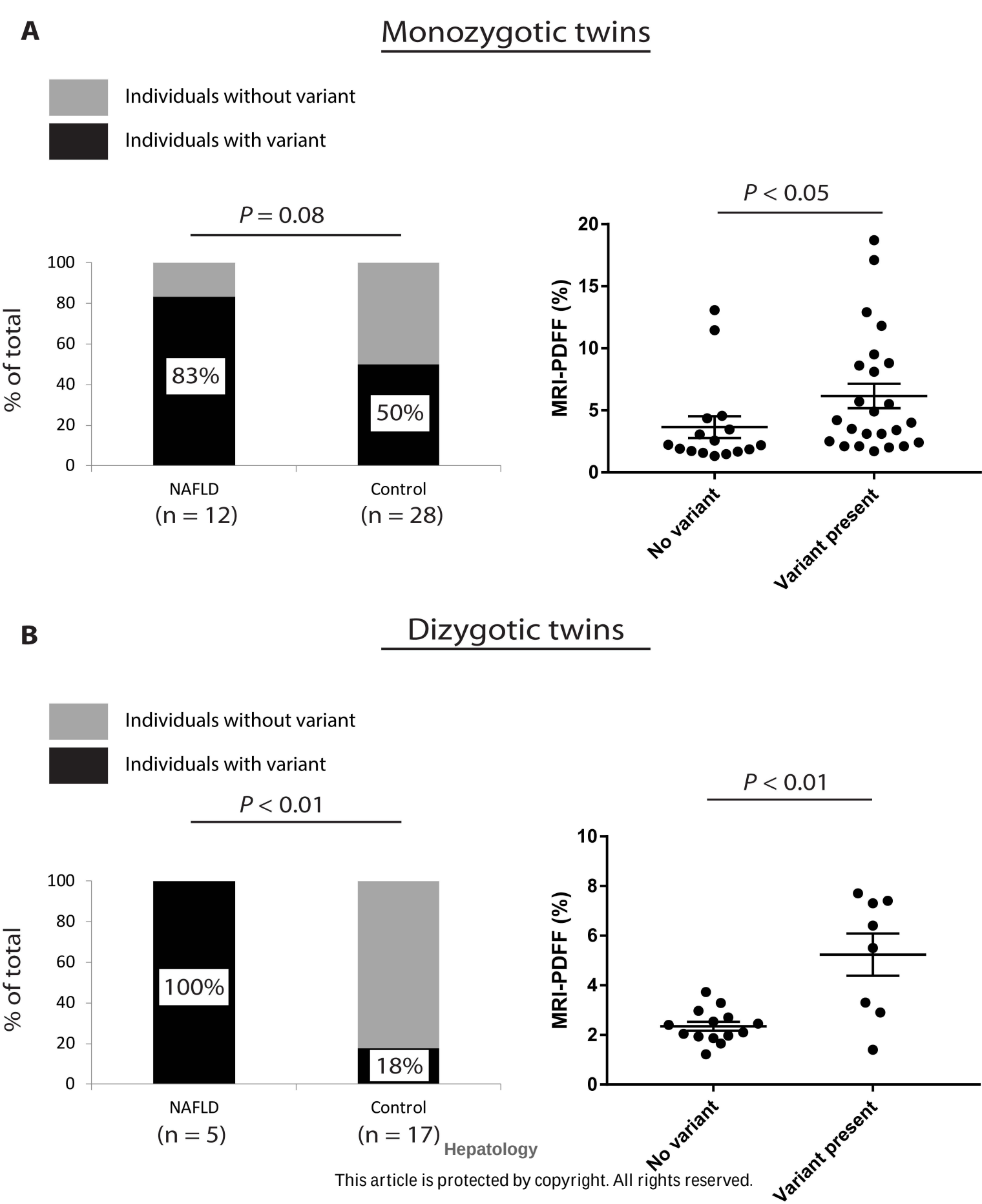

Fig. S4. Among both monozygotic (A) and dizygotic twins (B), variants in lamina-related genes were predominantly found in twins with NAFLD. (A) Monozygotic twin pairs (20 pairs, n=40 subjects). *Left panel*: Percentages of monozygotic twins (*y*-axis) with and without genetic variant(s) are shown for both NAFLD cases (n=12) and Controls (n=28) (includes all coding variants with minor allele frequency < 0.06). Fisher's exact test was used to assess statistical significance at a threshold of $P<0.05$. *Right panel:* Scatter plot of liver fat content (assessed by MRI-PDFF) of monozygotic twins without (n=16) and with (n=24) a lamina-related genetic variant (includes all coding variants with minor allele frequency < 0.06). Error bars represent standard error of the mean; Mann-Whitney U test was used to assess statistical significance at a threshold of $P<0.05$. (B) Dizygotic twin pairs (11 pairs, n=22 subjects). *Left panel*: Percentages of twins (*y*-axis) with and without genetic variant(s) are shown for both NAFLD cases (n=5) and Controls (n=17) (includes all coding variants with minor allele frequency < 0.06). Fisher's exact test was used to assess statistical significance at a threshold of $P<0.05$. *Right panel:* Scatter plot of liver fat content (assessed by MRI-PDFF) of twins without (n=14) and with (n=8) a lamina-related genetic variant (includes all coding variants with minor allele frequency < 0.06). Error bars represent standard error of the mean; Mann-Whitney U test was used to assess statistical significance at a threshold of $P<0.05$.

Fig S5

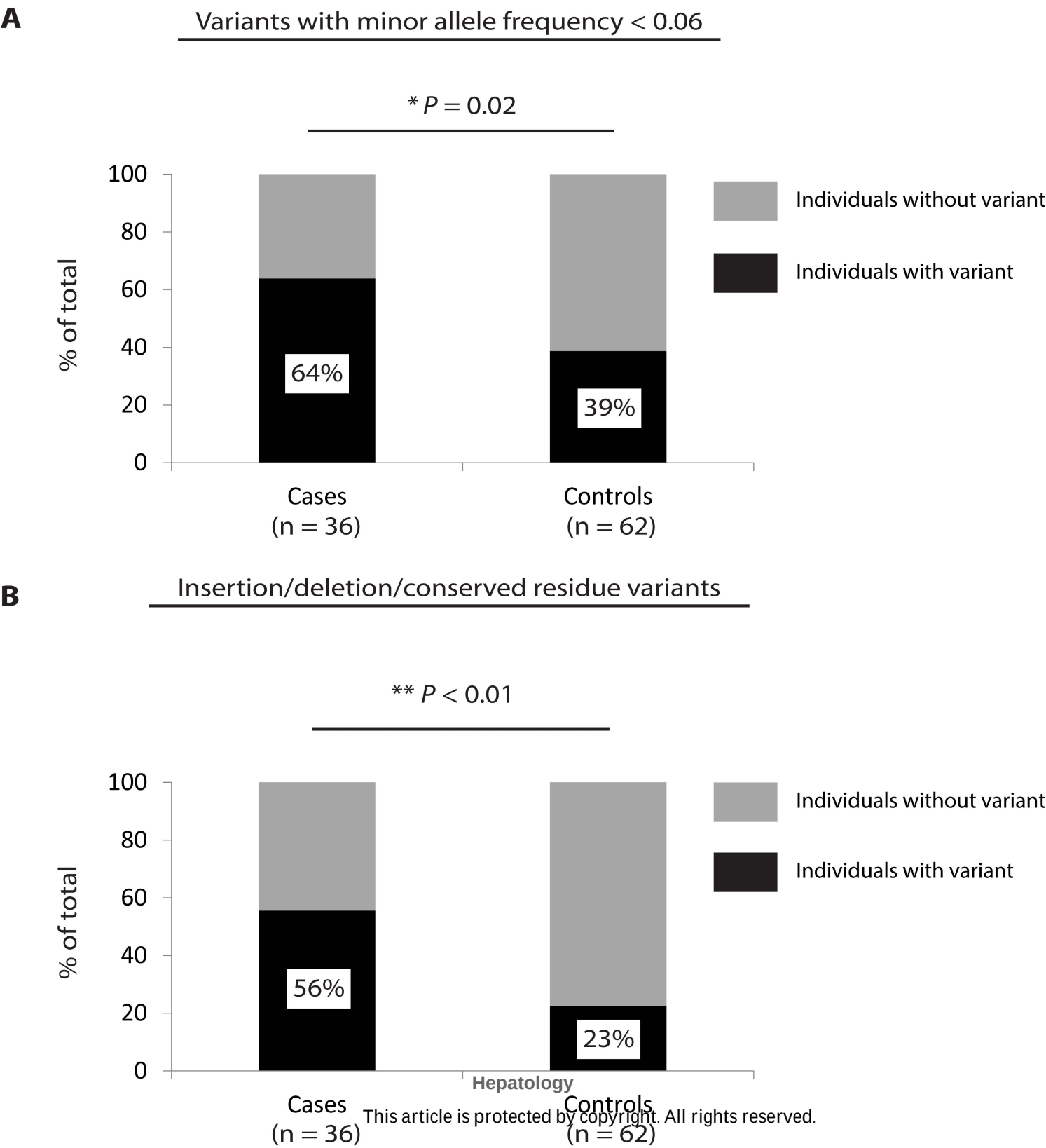

Fig. S5. Among all subjects (n=98), including both twin/sibling pairs (n=74) and additional subjects not part of a twin/sibling pair (n=24), variants in lamina-related genes were predominantly found in individuals with NAFLD. (A) Percentages of individuals (*y*-axis) with and without genetic variant(s) are shown for both NAFLD cases (n=36) and controls (n=62) (includes all coding variants with minor allele frequency < 0.06). (B) Percentages of individuals (*y*-axis) with and without a variant resulting in insertion/deletion or change in a conserved residue are shown for NAFLD cases (n=36) and controls (n=62). Fisher's exact test was used to assess statistical significance at a threshold of $P<0.05$.

Fig S6

A

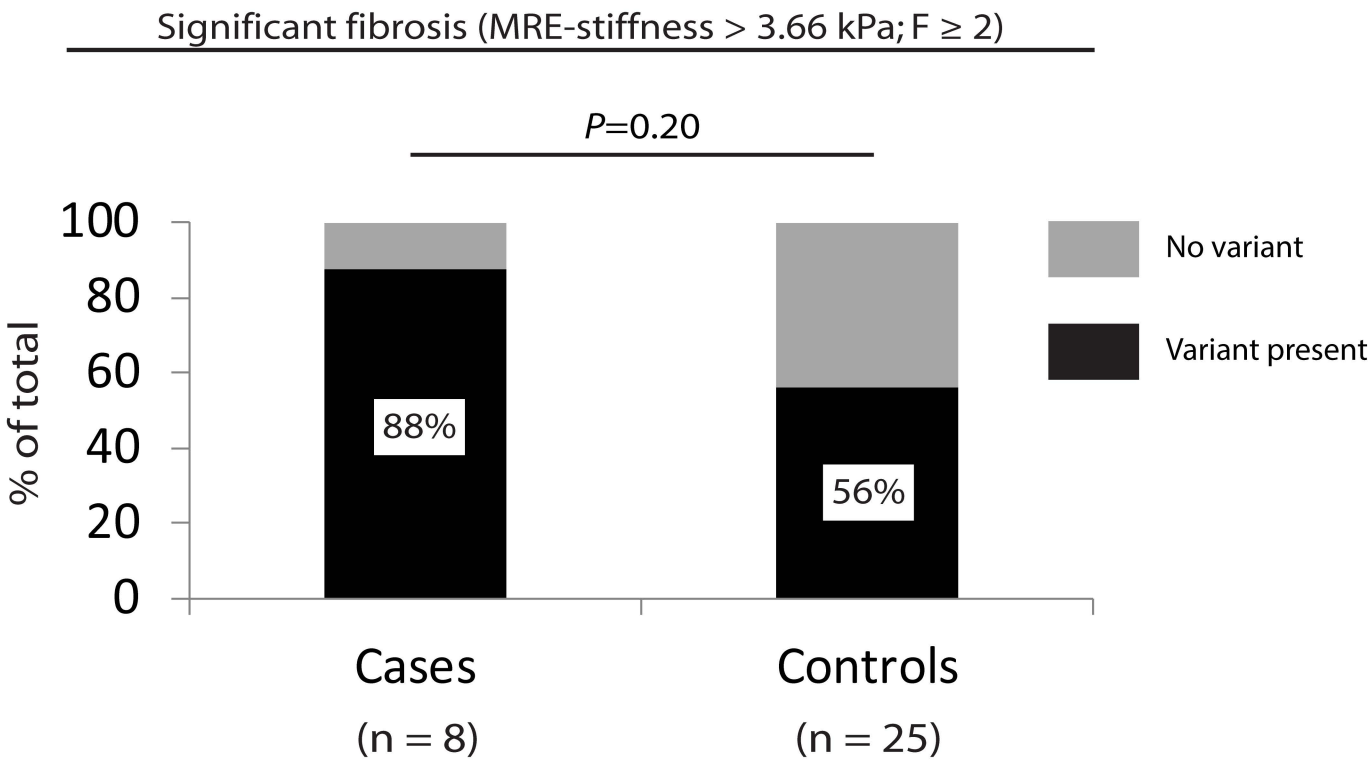

B

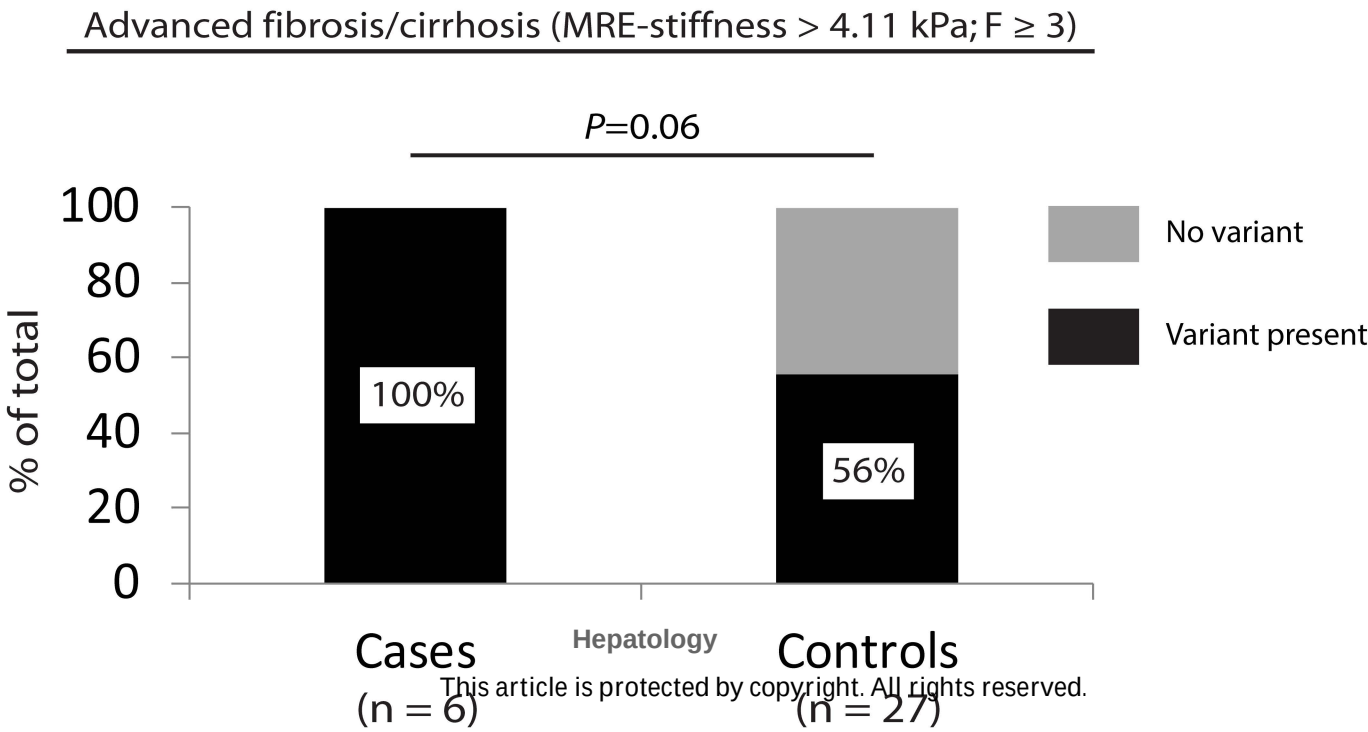

Fig. S6. Lamina-related variants among study participants with NAFLD and hepatic fibrosis. (A) Significant fibrosis: Percentages of individuals (*y*-axis) with and without genetic variant(s) are shown for both Cases (NAFLD with MRE > 3.66 kPa; F ≥ 2) and Controls (NAFLD with MRE < 3.66 kPa; F < 2). (B) Advanced fibrosis/cirrhosis: Percentages of individuals (*y*-axis) with and without genetic variant(s) are shown for both cases (NAFLD with MRE > 4.11 kPa; F ≥ 3) and controls (NAFLD with MRE < 4.11 kPa; F < 3). For each group, Fisher's exact test was used to assess statistical significance at a threshold of $P<0.05$. Note that this analysis includes twins and siblings with NAFLD (n=20 twins/siblings with NAFLD and MRE data) as well as additional subjects with NAFLD who were not part of a twin/sibling pair (n=13 subjects with NAFLD and MRE data); n=33 total subjects.

Fig S7

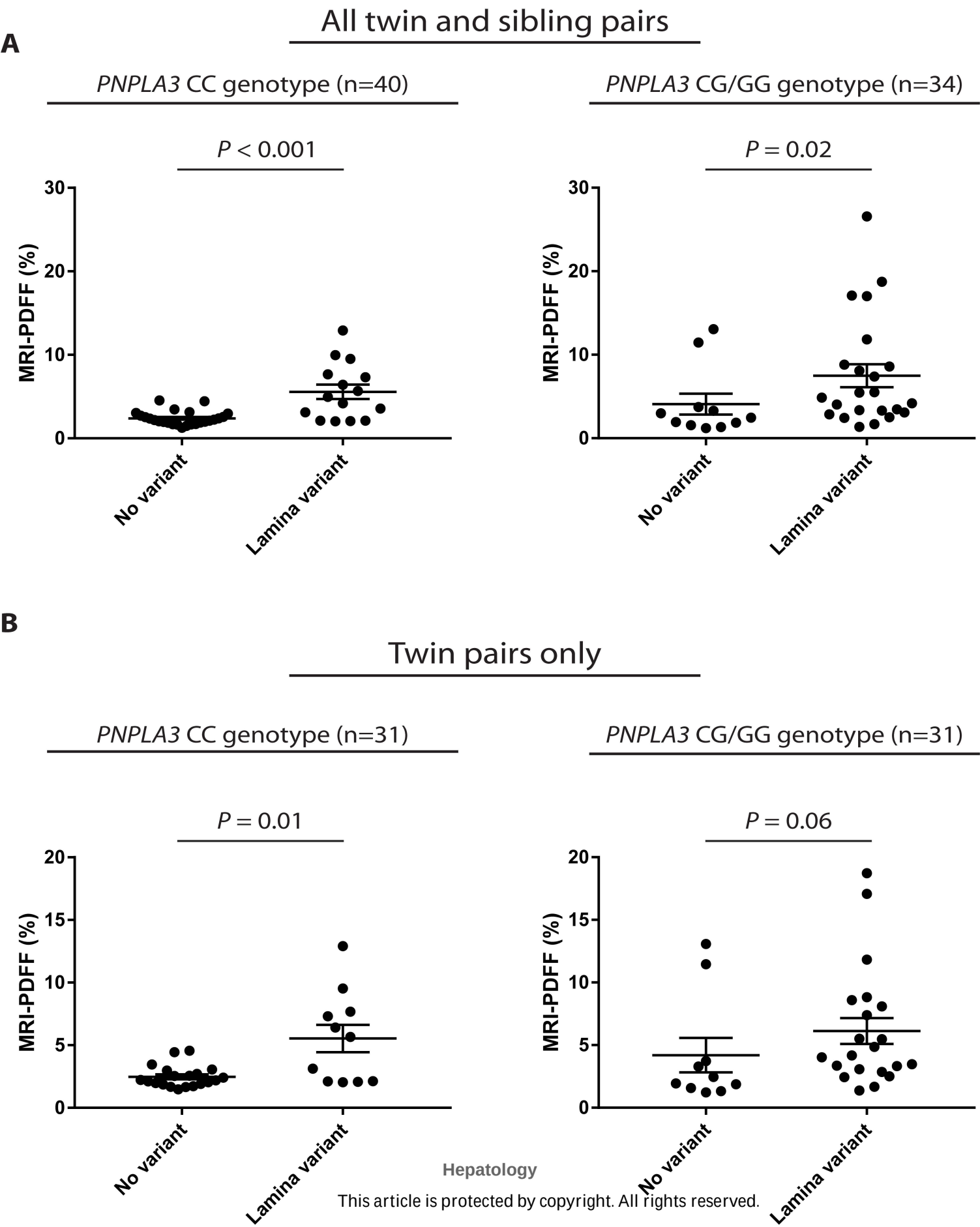

Fig. S7. Presence or absence of lamina-related genetic variants stratified by *PNPLA3* genotype. (A) All twin and sibling pairs (37 pairs, n=74 subjects). *Left panel*: Scatter plot of liver fat content (assessed by MRI-PDFF) of the 40 subjects with *PNPLA3* CC genotype without and with a lamina-related genetic variant. *Right panel*: Scatter plot of liver fat content (assessed by MRI-PDFF) of the 34 subjects with *PNPLA3* CG or GG genotype without and with a lamina-related genetic variant. Error bars represent standard error of the mean; Mann-Whitney U test was used to assess statistical significance at a threshold of $P<0.05$. (B) Twin pairs only (31 pairs, n=62 subjects). *Left panel*: Scatter plot of liver fat content (assessed by MRI-PDFF) of the 31 twins with *PNPLA3* CC genotype without and with a lamina-related genetic variant. *Right panel*: Scatter plot of liver fat content (assessed by MRI-PDFF) of the 31 twins with *PNPLA3* CG or GG genotype without and with a lamina-related genetic variant. Error bars represent standard error of the mean; Mann-Whitney U test was used to assess statistical significance at a threshold of $P<0.05$. Note that subjects with *PNPLA3* CG and GG genotypes were grouped for these analyses due to the small number of GG homozygotes (n=12) in the cohort.

Fig S8

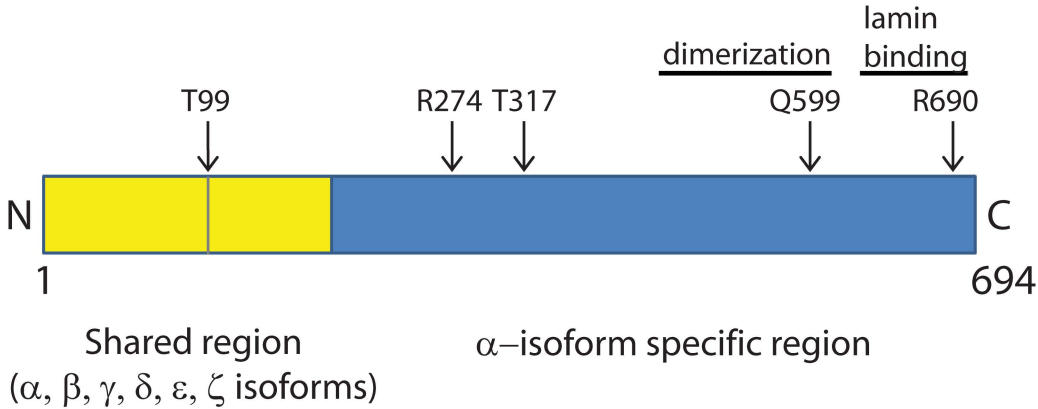

Fig. S8. Schematic of the LAP2α protein. The *TMPO* gene encodes six isoforms of LAP2, which are derived via alternative splicing. As shown, four of the five genetic variants in *TMPO* identified in this study were in the portion of the gene unique to the α isoform (blue shading), which is known to interact with lamin A. The fifth variant (within the yellow shading) was a single basepair insertion causing a frameshift and premature stop codon after Thr 99 in the translated protein.

Fig S9

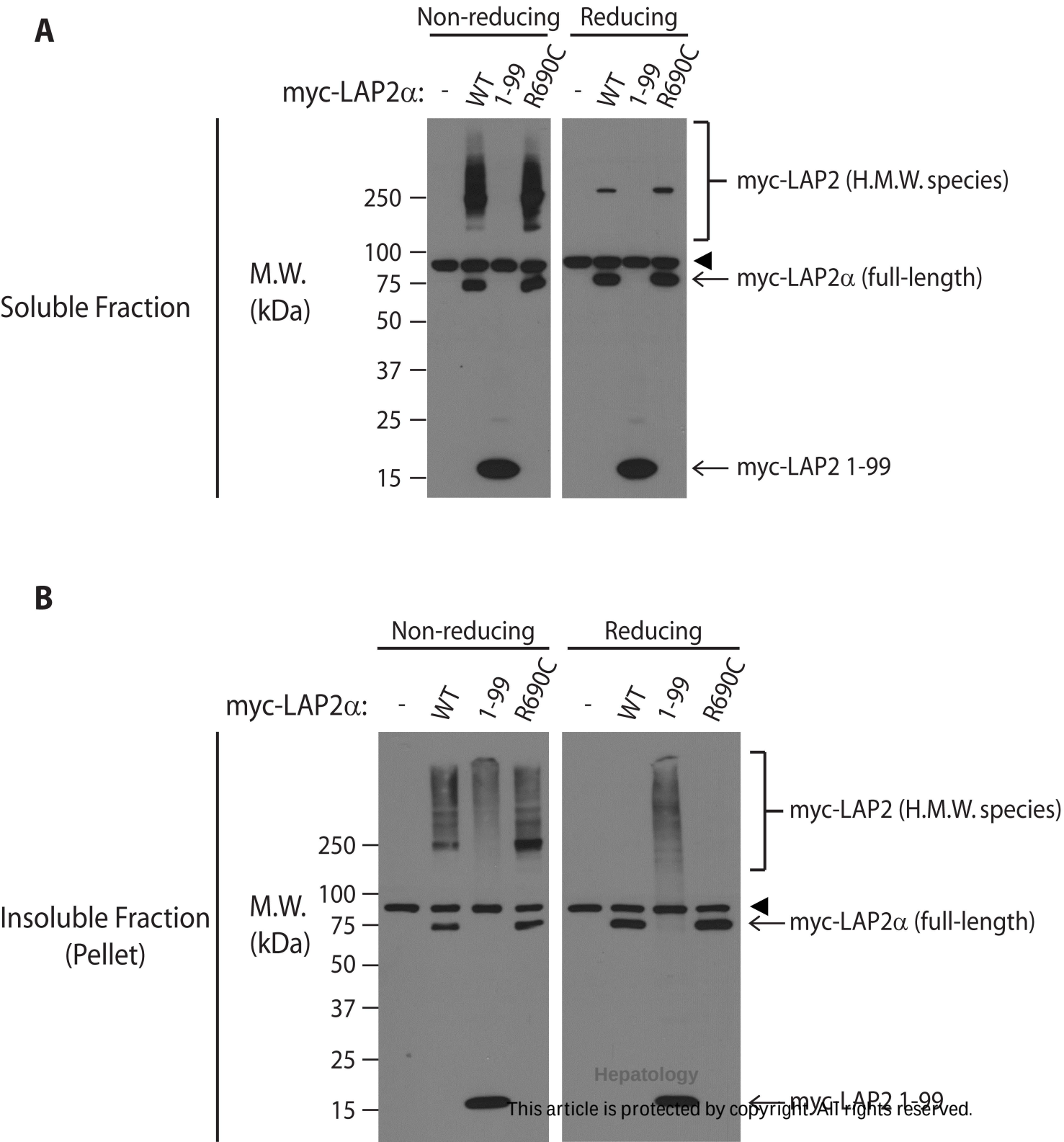

Fig. S9. Full-length, but not truncated, LAP2α forms a soluble high-molecular weight species under non-reducing conditions. (A) Huh7 cells were transfected with wild-type (WT) LAP2α or the indicated variant. Two days after transfection, cells were harvested and the Triton-soluble fraction was resolved on denaturing SDS-PAGE under non-reducing or reducing conditions. Transfected LAP2 was visualized by immunoblotting with antibody directed to the myc tag. (B) The Triton-insoluble (pellet) fraction of Huh7 cells, transfected as in panel A, was resolved using denaturing SDS-PAGE (non-reducing and reducing) and analyzed by immunoblotting. H.M.W., high molecular weight; M.W., apparent molecular weight; kDa, kilodaltons. Arrowhead highlights a non-specific band recognized by the myc antibody.

Fig S10

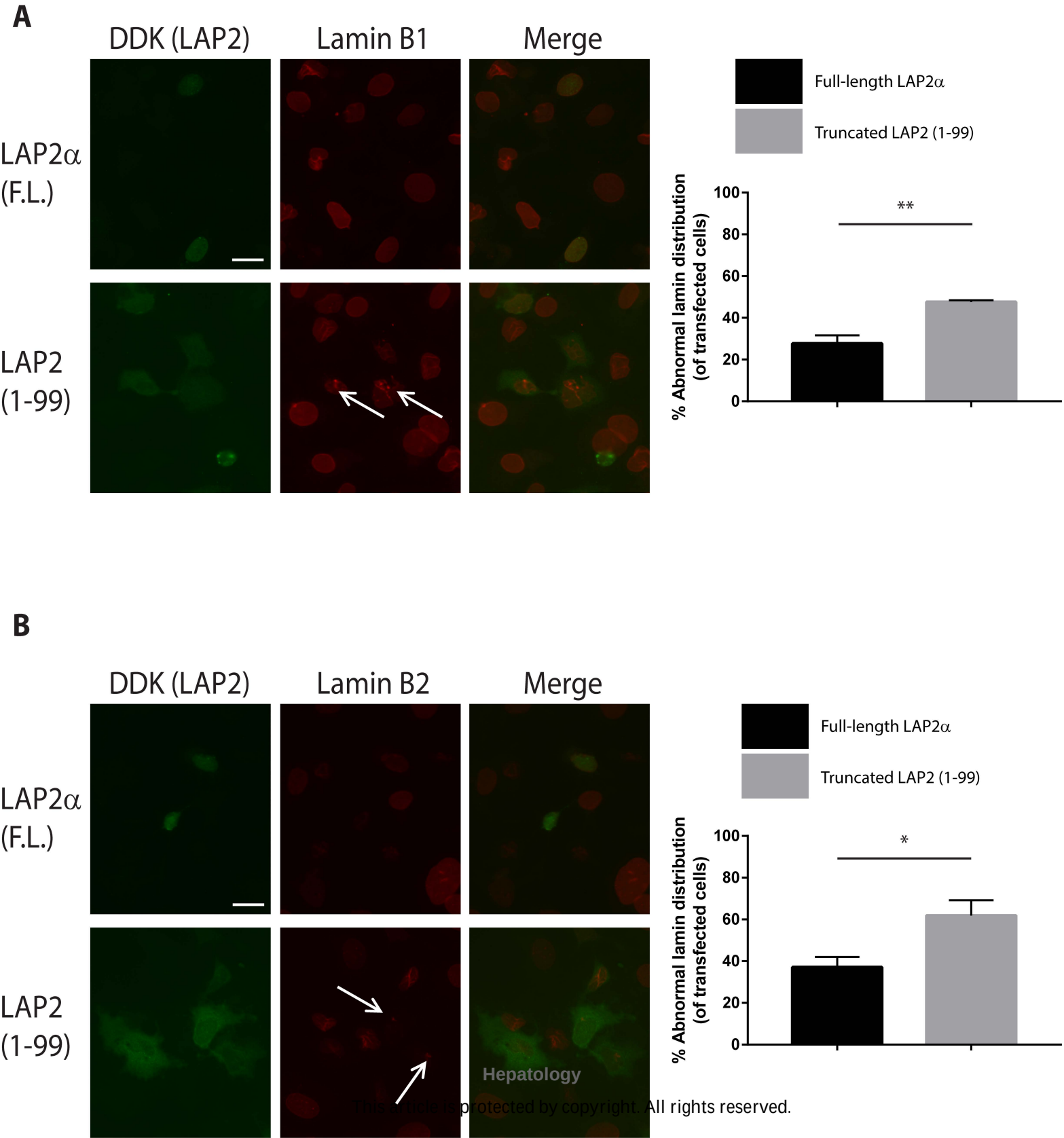

Fig. S10. Truncated LAP2 alters B-type lamin distribution. (A) Huh7 cells were transfected with DDK-tagged full-length (F.L.) LAP2α or truncated LAP2 (1-99). After fixation, transfected LAP2 and endogenous lamin B1 were visualized by immunofluorescence using anti-FLAG and anti-lamin B1 antibodies, respectively. Representative high-magnification images are shown; nuclei of transfected cells with abnormal lamin staining (punctate/globular) are indicated by arrows. Scale bar, 20 μm. Right panel shows quantitation (>40 nuclei scored for each condition). Error bars represent standard error of the mean. Student's *t* test was used to determine statistical significance; **, $P<0.01$. (B) Cells were transfected with full-length or truncated LAP2α with DDK tag as in panel A. After fixation, transfected LAP2 and endogenous lamin B2 were visualized by immunofluorescence using anti-FLAG and anti-lamin B2 antibodies, respectively. Representative high-magnification images are shown; nuclei of transfected cells with abnormal lamin staining (punctate/globular) are indicated by arrows. Scale bar, 20 μm. Right panel shows quantitation (>40 nuclei scored for each condition). Error bars represent standard error of the mean. Student's *t* test was used to determine statistical significance; *, $P<0.05$.

Primer Name	Variant	Sequence (5' → 3')
ZMPSTE24-L438F-FWD	*ZMPSTE24* L438F	TTTCTGGCCTGTTTGCTTGG
ZMPSTE24-L438F-REV	*ZMPSTE24* L438F	CATGCTGCCAGGACAGAAAT
BANF1-G21E-FWD	*BANF1* G21E	GGGAAGAGTCTCCCTGGAAC
BANF1-G21E-REV	*BANF1* G21E	TGCCATTCAGAGCACACAAG
TMPO-T99fs-FWD	*TMPO* T99fs	AGTTACTTGCTTGGCTGTGC
TMPO-T99fs-REV	*TMPO* T99fs	GTCCTTGGAACCTAAACTGCT
TMPO-R274K-FWD	*TMPO* R274K; *TMPO* T317S	TCTTGTTGCCACAAACTTGC
TMPO-R274K-REV	*TMPO* R274K; *TMPO* T317S	CCAGTGGGGGCATAGAGTTA
TMPO-Q599E-FWD	*TMPO* Q599E	TGGCATGCAAATATCCAGTTTC
TMPO-Q599E-REV	*TMPO* Q599E	AATCCTTCAGCCAGAGGTATCG
TMPO-R690C-FWD	*TMPO* R690C	CGCTTGGGATTCTGAGCAAA
TMPO-R690C-REV	*TMPO* R690C	ATTGTTTGTACCAGGCTTCCT
SREBF1-V610M-FWD	*SREBF1* V610M	GGGACAGATTCATGGTGTGCACAGG
SREBF1-V610M-REV	*SREBF1* V610M	GAACTTGGGGCTCTGGATTTCCTGG
SREBF2-S72ins-FWD	*SREBF2* S72ins	GAAAGAGGTAAGGGTTTCCTGACCC
SREBF2-S72ins-REV	*SREBF2* S72ins	CTTGACTTGCAGAGTTGGAGCCTGTG
SREBF2-R371K-FWD	*SREBF2* R371K	TAACTTCTCCCGAGTGGCAC
SREBF2-R371K-REV	*SREBF2* R371K	CCACCTCATTGTCCACCAGA
SREBF2-G595A-FWD	*SREBF2* G595A	GGAAATACCTCAGAATGTCAGCAGGG
SREBF2-G595A-REV	*SREBF2* G595A	GCTGGTCTTAGCTTCGTCTTCAAAGC
SREBF2-R860S-FWD	*SREBF2* R860S	GGTCTTAGAGCTGGAGAGCTGAACAG
SREBF2-R860S-REV	*SREBF2* R860S	GAACTGGAGCCACAGGTATGAACCTG
SREBF2-R1080Q-FWD	*SREBF2* R1080Q	CTTTTCCGTGGATTGGGTGG
SREBF2-R1080Q-REV	*SREBF2* R1080Q	CCACTCTCAGCGGGAAGAT

Table S1. Primers used for PCR amplification of genomic DNA and Sanger sequencing.

Antibody target	Manufacturer	Catalog/clone number	Dilution
FLAG / DDK tag	Sigma-Aldrich	F1804 (clone M2)	1:250 (IF)
GFP	Origene	TA150041 (clone 2H8)	1:2000 (IB); 1.5 µg per 500 µL lysate (IP)
Myc tag	Abcam	ab9106	1:1000 (IB)
Lamin A/C	Santa Cruz Biotechnology	sc-20681 (H-110)	1:250 (IF)
Lamin B1	Abcam	ab16048	1:250 (IF)
Lamin B2	Cell Signaling	12255 (clone D8P3U)	1:250 (IF)
p62/SQSTM1	Abcam	ab96706	1:2000 (IB)

Table S2. Antibodies used for immunofluorescence (IF), immunoprecipitation (IP), and immunoblotting (IB).

Gene	Protein	Associated disease(s)
LMNA	A-type lamin	Dilated cardiomyopathy, progeria, lipodystrophy, Charcot-Marie-Tooth disease, muscular dystrophy (1-9)
LMNB2	B-type lamin	Lipodystrophy (10)
ZMPSTE24	Lamin-processing enzyme	Mandibuloacral dysplasia, lipodystrophy, restrictive dermopathy (11, 12)
ICMT	Lamin-processing enzyme	None known
FNTA	Lamin-processing enzyme	None known
FNTB	Lamin-processing enzyme	None known
TMPO	Lamin binding partner	Dilated cardiomyopathy (13)
BANF1	Lamin binding partner	Atypical progeria (14)
SREBF1	Transcription factor	None known
SREBF2	Transcription factor	None known

Table S3. Candidate genes sequenced.

Table S4. LAP2 interacting proteins as determined by mass spectrometry (appended separately).

TWIN ID	Sex	Age (yrs)	NAFLD	Diabetes	Other chronic disease	*PNPLA3* genotype	Height (m)	Weight (kg)	BMI (kg/ m^2)	Alcohol use	ALT (IU/L)	Glucose (mg/dL)	Insulin (µU/mL)	HOMA-IR	TG (mg/dL)
TW01	M	41	No	No	No	CG	1.73	83.9	28	None	26	92	8	1.8	79
TW02	M	41	Yes	No	No	CG	1.74	100.6	33	Rare (less than once per week)	26	90	14	3.1	172

Table S5. Clinical and laboratory data for monozygotic twins TW01 and TW02 carrying insertion in *TMPO*. U, units; IU, international units; HOMA-IR, homeostatic model of insulin resistance; TG, triglycerides.

Supplementary Methods

Study participant recruitment and clinical data acquisition. All participants (recruited between January 2012 and January 2015) underwent a standardized clinical research visit at the University of California San Diego (UCSD) NAFLD Translational Research Unit including detailed medical history, assessment of alcohol consumption, physical examination, testing to exclude other causes of chronic liver disease, fasting laboratory tests (see below), and magnetic resonance imaging (MRI) examination of the liver. Research visits and MRI procedures for each related pair were performed on the same day. The Alcohol Use Disorders Identification Test questionnaire and Skinner Lifetime Drinking history were administered to record and quantify alcohol use. A physical examination including vital signs, height, weight, and anthropometric measurements was performed. Body mass index (BMI) was calculated by dividing body weight by the square of the height (kilogram/meters^2). Fasting laboratory studies were obtained for all participants including complete blood count, liver disease screening tests (hepatitis B surface antigen, hepatitis C antibody, and iron panel including serum ferritin), clinical chemistry (creatinine, total protein, blood urea nitrogen, uric acid), hemoglobin A1c, hepatic panel (total bilirubin, direct bilirubin, aspartate aminotransferase, alanine aminotransferase [ALT], alkaline phosphatase, γ-glutamyltransferase, albumin, prothrombin time, and international normalized ratio), lipid profile, and glucose/insulin levels. MRI examinations were performed using a 3T research scanner (GE Signa EXCITE HDxt; GE Healthcare, Waukesha, WI) at the UCSD MR3T Research Laboratory. Liver fat was measured via MRI-determined proton-density fat-fraction (MRI-PDFF), and liver fibrosis was quantified by MR elastography-determined stiffness (MRE-stiffness) as described (15). NAFLD was defined as MRI-PDFF ≥5%

without apparent secondary cause of hepatic steatosis such as significant alcohol use, use of steatogenic medication(s), or other cause of liver disease.

Next-generation DNA sequencing and variant identification: Next-generation sequence data was obtained from genomic DNA by amplification of target regions with a custom Illumina TruSeq amplicon panel and analysis via Illumina MiSeq instrument. Sequences were then trimmed using Trimmomatic v0.32 and aligned to human reference genome build Grc37/hg19 using the Burrows-Wheeler Aligner 'mem' algorithm v0.7.8. Variants were detected using the Broad Institute Genome Analysis Toolkit v.3.3-0 Haplotype Caller with default parameters, -strand_emit_conf 10 and -strand_call_conf 30, DISCOVERY mode. Variant filtering, annotation and reporting were performed using VarSeq v.1.1.0 (Golden Helix, Bozeman, MT). Variants with fewer than 5 alternate observations were removed. Variants were annotated based on RefSeq v.69 gene models, and matched with 1000 Genomes Phase 3 population frequency data and dbNSFP v2.0 functional annotations (16, 17).

Supplementary References

1. Worman HJ, Fong LG, Muchir A, Young SG. Laminopathies and the long strange trip from basic cell biology to therapy. J Clin Invest 2009;119:1825-1836.

2. Davidson PM, Lammerding J. Broken nuclei--lamins, nuclear mechanics, and disease. Trends Cell Biol 2014;24:247-256.

3. Hatch E, Hetzer M. Breaching the nuclear envelope in development and disease. J Cell Biol 2014;205:133-141.

4. Taylor MR, Fain PR, Sinagra G, Robinson ML, Robertson AD, Carniel E, Di Lenarda A, et al. Natural history of dilated cardiomyopathy due to lamin A/C gene mutations. J Am Coll Cardiol 2003;41:771-780.

5. **Van Esch H, Agarwal AK**, Debeer P, Fryns JP, Garg A. A homozygous mutation in the lamin A/C gene associated with a novel syndrome of arthropathy, tendinous calcinosis, and progeroid features. J Clin Endocrinol Metab 2006;91:517-521.

6. Guenantin AC, Briand N, Bidault G, Afonso P, Bereziat V, Vatier C, Lascols O, et al. Nuclear envelope-related lipodystrophies. Semin Cell Dev Biol 2014;29:148-157.

7. Bonne G, Di Barletta MR, Varnous S, Becane HM, Hammouda EH, Merlini L, Muntoni F, et al. Mutations in the gene encoding lamin A/C cause autosomal dominant Emery-Dreifuss muscular dystrophy. Nat Genet 1999;21:285-288.

8. Fatkin D, MacRae C, Sasaki T, Wolff MR, Porcu M, Frenneaux M, Atherton J, et al. Missense mutations in the rod domain of the lamin A/C gene as causes of dilated cardiomyopathy and conduction-system disease. N Engl J Med 1999;341:1715-1724.

9. Ajluni N, Meral R, Neidert AH, Brady GF, Buras E, McKenna B, DiPaola F, et al. Spectrum of disease associated with partial lipodystrophy: lessons from a trial cohort. Clin Endocrinol (Oxf) 2017;86:698-707.

10. Hegele RA, Cao H, Liu DM, Costain GA, Charlton-Menys V, Rodger NW, Durrington PN. Sequencing of the reannotated LMNB2 gene reveals novel mutations in patients with acquired partial lipodystrophy. Am J Hum Genet 2006;79:383-389.

11. Agarwal AK, Fryns JP, Auchus RJ, Garg A. Zinc metalloproteinase, ZMPSTE24, is mutated in mandibuloacral dysplasia. Hum Mol Genet 2003;12:1995-2001.

12. Navarro CL, De Sandre-Giovannoli A, Bernard R, Boccaccio I, Boyer A, Genevieve D, Hadj-Rabia S, et al. Lamin A and ZMPSTE24 (FACE-1) defects cause nuclear disorganization and identify restrictive dermopathy as a lethal neonatal laminopathy. Hum Mol Genet 2004;13:2493-2503.

13. Taylor MR, Slavov D, Gajewski A, Vlcek S, Ku L, Fain PR, Carniel E, et al. Thymopoietin (lamina-associated polypeptide 2) gene mutation associated with dilated cardiomyopathy. Hum Mutat 2005;26:566-574.

14. Puente XS, Quesada V, Osorio FG, Cabanillas R, Cadinanos J, Fraile JM, Ordonez GR, et al. Exome sequencing and functional analysis identifies BANF1 mutation as the cause of a hereditary progeroid syndrome. Am J Hum Genet 2011;88:650-656.

15. Loomba R, Schork N, Chen CH, Bettencourt R, Bhatt A, Ang B, Nguyen P, et al. Heritability of Hepatic Fibrosis and Steatosis Based on a Prospective Twin Study. Gastroenterology 2015;149:1784-1793.

16. 1000 Genomes Project Consortium (Auton A, Brooks LD, Durbin RM, Garrison EP, Kang HM, Korbel JO, et al.). A global reference for human genetic variation. Nature 2015;526:68-74.

17. Liu X, Jian X, Boerwinkle E. dbNSFP v2.0: a database of human non-synonymous SNVs and their functional predictions and annotations. Hum Mutat 2013;34:E2393-2402.

Supplementary Table 4. LAP2-interacting proteins. GFP-tagged LAP2α (full-leng
to LC-MS/MS analysis after in-solution trypsin digestion as described in Material a
peptide-specific spectra, and proteins with fewer than 15 spectra (with either full-le
ratio of peptide-specific spectra with truncated LAP2 (1-99) to peptide-specific spe
with LAP2 1-99.

Accession	Description	% Coverage	# Peptides	# Peptide spectrum r
Q13501-1	sequestosome-1 [OS=Homo s	63.9	13	39
Q9Y4L1	Hypoxia up-regulated protein	46.3	34	82
Q14697-1	Neutral alpha-glucosidase AB	39.4	25	61
Q9H936	Mitochondrial glutamate carrie	39.3	9	18
P02675	Fibrinogen beta chain [OS=Ho	38.3	12	26
P07237	Protein disulfide-isomerase [O	37.6	14	30
P14866	Heterogeneous nuclear ribonu	34.3	14	31
O14967	calmegin [OS=Homo sapiens]	30.0	11	18
Q8N163-1	Cell cycle and apoptosis regul	28.4	15	34
P17812	CTP synthase 1 [OS=Homo sa	27.4	11	23
P40939	Trifunctional enzyme subunit a	25.0	12	34
P08195-4	Isoform 4 of 4F2 cell-surface a	24.8	12	23
P10909-2	Isoform 2 of Clusterin [OS=Ho	23.0	9	19
P00367	Glutamate dehydrogenase 1,	22.4	10	17
P27824-2	Isoform 2 of Calnexin [OS=Ho	21.7	11	25
O15027-5	Isoform 5 of Protein transport	20.9	29	63
Q9NVH1-1	DnaJ homolog subfamily C me	20.8	9	15
P27708	CAD protein [OS=Homo sapie	20.7	33	78
O94832	Unconventional myosin-Id [OS	16.9	15	40
P05023	Sodium/potassium-transportin	16.5	12	22
P55157	microsomal triglyceride transfe	16.2	11	19
Q8NBJ5	Procollagen galactosyltransfer	15.6	9	16
Q92614-1	Unconventional myosin-XVIIIa	15.4	24	50
Q86VP6-1	cullin-associated nedd8-dissoc	14.4	12	21
Q92616	eIF-2-alpha kinase activator G	14.2	26	45
P04114	apolipoprotein B-100 [OS=Hor	13.5	48	83
Q9BQG0-2	Isoform 2 of Myb-binding prote	12.1	10	26
Q09666-1	Neuroblast differentiation-asso	11.3	12	30
Q7Z6Z7	E3 ubiquitin-protein ligase HU	10.3	29	44
Q6P2E9-1	Enhancer of mRNA-decapping	9.9	9	19
P42704	Leucine-rich PPR motif-contai	7.7	9	17
Q96CS3	FAS-associated factor 2 [OS=	46.3	12	30
Q13200	26S proteasome non-ATPase	24.3	16	36
O94973-2	Isoform 2 of AP-2 complex sub	21.7	16	42
P54136-1	arginine--tRNA ligase, cytopla	41.5	22	57
Q86TG7-1	Retrotransposon-derived prote	30.4	12	34
Q9Y285	Phenylalanine--tRNA ligase al	41.9	15	41
O60762	Dolichol-phosphate mannosylt	43.8	8	19
Q99848	Probable rRNA-processing pro	36.6	11	42
P41250	Glycine--tRNA ligase [OS=Hor	25.0	14	29
Q9Y512	sorting and assembly machine	22.2	8	18
O95864	fatty acid desaturase 2 [OS=H	20.0	7	22

Q9UBX3-2	Isoform 2 of Mitochondrial dica	53.7	11	26
Q02978	Mitochondrial 2-oxoglutarate/n	24.2	7	20
P56192	Methionine--tRNA ligase, cyto	30.3	17	38
O95433	activator of 90 kDa heat shock	45.9	11	24
Q13813-2	Isoform 2 of Spectrin alpha ch	20.3	39	96
P47897	glutamine--tRNA ligase [OS=H	43.9	24	68
P35998	26S protease regulatory subur	31.6	10	22
O60701	UDP-glucose 6-dehydrogenas	51.6	16	47
O95573	long-chain-fatty-acid--CoA liga	37.5	20	45
P28331-2	Isoform 2 of NADH-ubiquinone	26.0	12	21
Q15392	Delta(24)-sterol reductase [OS	21.3	10	21
P51812	Ribosomal protein S6 kinase a	19.3	10	21
Q96PK6-1	RNA-binding protein 14 [OS=H	26.9	13	38
P49368-1	T-complex protein 1 subunit ga	43.3	18	63
P41252	isoleucine--tRNA ligase, cytop	28.4	30	80
P07814	Bifunctional glutamate/proline-	39.5	44	136
P50454	Serpin H1 [OS=Homo sapiens	48.6	15	39
P46777	60S ribosomal protein L5 [OS=	35.0	8	43
Q05682-3	Isoform 3 of Caldesmon [OS=	27.6	12	42
P31689-1	DnaJ homolog subfamily A me	44.8	11	27
Q9UBS4	DnaJ homolog subfamily B me	35.5	10	26
Q06210-1	glutamine--fructose-6-phospha	48.6	25	60
Q9UM54-6	Isoform 6 of Unconventional m	36.6	34	97
P16989-1	Y-box-binding protein 3 [OS=H	19.9	6	50
P78527	DNA-dependent protein kinase	36.0	113	351
P78371-1	T-complex protein 1 subunit be	39.8	15	53
P06576	ATP synthase subunit beta, m	49.1	18	56
P16615	Sarcoplasmic/endoplasmic ret	24.3	19	48
P32969	60S ribosomal protein L9 [OS=	61.5	8	48
Q16891-2	Isoform 2 of MICOS complex s	39.2	22	70
P63010-2	Isoform 2 of AP-2 complex sub	38.7	26	82
O95782	AP-2 complex subunit alpha-1	25.8	21	63
Q9NVI7-2	Isoform 2 of ATPase family AA	32.3	18	67
P17987	T-complex protein 1 subunit al	61.0	25	104
Q13148-1	TAR DNA-binding protein 43 [	35.5	8	22
P43243	Matrin-3 [OS=Homo sapiens]	28.5	18	55
O75746	Calcium-binding mitochondrial	19.2	11	29
Q8WWM7-1	ataxin-2-like protein [OS=Hom	25.5	22	60
O00159-1	Unconventional myosin-Ic [OS	23.8	19	57
P14868	Aspartate--tRNA ligase, cytopl	47.1	21	66
O75874	Isocitrate dehydrogenase [NAI	30.7	10	29
P53621-1	coatomer subunit alpha [OS=H	32.5	33	93
Q9Y608	Leucine-rich repeat flightless-i	29.1	14	61
P55072	Transitional endoplasmic retic	57.8	34	139
P59998-3	Isoform 3 of Actin-related prote	54.5	8	46
Q9Y3I0	tRNA-splicing ligase RtcB hom	42.8	17	46
O15143	Actin-related protein 2/3 comp	34.7	9	42
Q9NYL9	tropomodulin-3 [OS=Homo sa	79.0	23	152
P33992	DNA replication licensing facto	36.6	19	52

P11498	pyruvate carboxylase, mitocho	32.6	27	81
P62917	60S ribosomal protein L8 [OS=	52.5	10	83
P50990	T-complex protein 1 subunit th	37.2	17	50
P48643	T-complex protein 1 subunit ep	36.2	16	52
P53007	Tricarboxylate transport protei	42.8	9	35
P49327	Fatty acid synthase [OS=Hom	36.2	61	219
Q00325-2	Isoform B of Phosphate carrie	42.4	15	56
P14649	Myosin light chain 6B [OS=Ho	40.4	7	56
Q92499	ATP-dependent RNA helicase	37.2	20	66
Q04637-9	Isoform 9 of Eukaryotic transla	16.5	20	63
O43795	Unconventional myosin-Ib [OS	45.7	43	184
Q15366-3	Isoform 3 of Poly(rC)-binding p	37.6	10	46
P07900-2	Isoform 2 of Heat shock protei	33.0	22	88
P62841	40S ribosomal protein S15 [OS	69.7	7	61
Q15365	Poly(RC)-binding protein 1 [OS	41.3	11	41
P67809	Nuclease-sensitive element-bi	53.4	11	73
Q92598	Heat shock protein 105 kDa [O	33.1	20	75
P25205-2	Isoform 2 of DNA replication li	24.7	16	54
O75643-1	U5 small nuclear ribonucleopr	19.1	30	75
P05362	Intercellular adhesion molecul	29.5	12	38
Q12906-7	Isoform 7 of Interleukin enhan	24.6	19	84
P50991	T-complex protein 1 subunit de	48.8	20	75
Q07065	Cytoskeleton-associated prote	40.7	18	63
Q8NBQ5	Estradiol 17-beta-dehydrogena	33.0	8	32
Q9Y224	UPF0568 protein C14orf166 [O	67.2	14	58
P07226-1	Tropomyosin alpha-4 chain [O	50.0	14	77
Q08211	Atp-dependent rna helicase a	33.0	31	110
P06753-2	Isoform 2 of Tropomyosin alph	45.6	14	61
P04843	Dolichyl-diphosphooligosaccha	39.9	17	63
P62888	60S ribosomal protein L30 [OS	67.0	7	82
P83731	60S ribosomal protein L24 [OS	37.6	7	40
P62136-2	Isoform 2 of Serine/threonine-	31.1	8	32
P00966	Argininosuccinate synthase [O	31.1	9	29
P18124	60S ribosomal protein L7 [OS=	52.0	16	102
P52272	Heterogeneous nuclear ribonu	64.1	32	219
P39023	60S ribosomal protein L3 [OS=	41.2	16	120
P26599-3	Isoform 3 of Polypyrimidine tra	54.6	18	111
P18621-3	Isoform 3 of 60S ribosomal pro	40.8	10	61
P61160-1	Actin-related protein 2 [OS=Ho	43.9	13	98
O15144	Actin-related protein 2/3 comp	63.3	14	76
Q9Y265	RuvB-like 1 [OS=Homo sapien	59.2	19	69
O75477	erlin-1 [OS=Homo sapiens]	28.9	8	29
Q6P2Q9	Pre-mRNA-processing-splicing	12.7	20	53
O43175	D-3-phosphoglycerate dehydro	25.1	10	32
P23528	Cofilin-1 [OS=Homo sapiens]	57.2	9	39
P61158	actin-related protein 3 [OS=Ho	73.0	20	135
P15880	40S ribosomal protein S2 [OS=	47.1	12	65
O94905-1	Erlin-2 [OS=Homo sapiens]	49.9	13	52
P62906	60S ribosomal protein L10A [O	53.0	14	109

Q9BQE3	Tubulin alpha-1C chain [OS=H	78.8	23	212
Q7Z406-6	Isoform 6 of Myosin-14 [OS=H	46.6	78	361
P08708	40S ribosomal protein S17 [OS	57.0	7	45
P62701	40S ribosomal protein S4, X is	51.3	15	108
Q9P2E9-1	Ribosome-binding protein 1 [O	68.3	73	355
P62241	40S ribosomal protein S8 [OS	51.9	11	84
P62424	60S ribosomal protein L7a [OS	54.1	19	130
P35580-4	Isoform 4 of Myosin-10 [OS=H	54.7	107	714
P27348	14-3-3 protein theta [OS=Hom	45.3	11	44
P35580-3	Isoform 3 of Myosin-10 [OS=H	54.5	106	711
P09651-1	Heterogeneous nuclear ribonu	28.8	9	40
P51991-1	Heterogeneous nuclear ribonu	28.0	9	42
P52597	Heterogeneous nuclear ribonu	25.1	7	31
P07951-2	Isoform 2 of Tropomyosin beta	53.5	15	72
P09493-3	Isoform 3 of Tropomyosin alph	49.3	15	70
P33993-1	DNA replication licensing facto	38.7	22	77
P08670	Vimentin [OS=Homo sapiens]	48.3	21	83
P61247	40S ribosomal protein S3a [OS	50.0	13	88
P09327	Villin-1 [OS=Homo sapiens]	51.6	32	241
Q00610-1	Clathrin heavy chain 1 [OS=H	55.5	69	383
P31943	Heterogeneous nuclear ribonu	44.1	13	82
P17066	Heat shock 70 kDa protein 6 [	20.2	14	124
P62750	60S ribosomal protein L23a [O	34.6	8	50
P11021	78 kDa glucose-regulated prot	60.1	34	269
P10809	60 kDa heat shock protein, mi	67.7	29	195
P17844	probable ATP-dependent RNA	51.0	25	128
O00571	ATP-dependent RNA helicase	48.6	25	124
P60709	Actin, cytoplasmic 1 [OS=Hom	74.9	20	542
P35579-1	Myosin-9 [OS=Homo sapiens]	60.9	131	1421
P27635	60S ribosomal protein L10 [OS	43.0	9	49
P62258-1	14-3-3 protein epsilon [OS=Ho	40.8	9	42
P09493-5	Isoform 5 of Tropomyosin alph	25.7	7	42
P60842	Eukaryotic initiation factor 4A-	67.2	23	117
P10412	Histone H1.4 [OS=Homo sapie	37.4	12	59
Q92841	Probable ATP-dependent RNA	35.9	23	112
P62244	40S ribosomal protein S15a [O	51.5	6	56
P36578	60S ribosomal protein L4 [OS=	42.4	18	145
Q9Y230	RuvB-like 2 [OS=Homo sapien	42.5	16	81
Q12905	Interleukin enhancer-binding fa	51.3	13	73
Q9BUJ2-1	Heterogeneous nuclear ribonu	22.0	12	51
P38919	Eukaryotic initiation factor 4A-	34.5	12	49
P62266	40S ribosomal protein S23 [OS	49.0	7	43
PRDX1_HUM	COMMON CONTAMINANT!	72.9	13	65
Q00839	Heterogeneous nuclear ribonu	28.5	17	105
Q02878	60S ribosomal protein L6 [OS=	49.7	15	125
P07910-2	Isoform C1 of Heterogeneous	41.6	14	88
P30050-1	60S ribosomal protein L12 [OS	54.5	6	90
P11940-1	Polyadenylate-binding protein	47.3	24	160
Q9NZI8	Insulin-like growth factor 2 mR	48.7	25	167

Q00839-2	Isoform Short of Heterogeneou	28.0	17	106
P05387	60S acidic ribosomal protein P	78.3	9	144
Q14240-2	Isoform 2 of Eukaryotic initiatio	32.8	10	49
P46781	40S ribosomal protein S9 [OS	40.2	9	59
P62269	40S ribosomal protein S18 [OS	52.6	11	79
P61978-2	Isoform 2 of Heterogeneous n	53.7	20	150
P60228	Eukaryotic translation initiation	34.8	13	67
P19338	Nucleolin [OS=Homo sapiens]	32.7	24	129
P61353	60S ribosomal protein L27 [OS	41.9	5	60
P09874	Poly [ADP-ribose] polymerase	36.0	29	114
P62280	40S ribosomal protein S11 [OS	46.8	8	63
P26373-1	60S ribosomal protein L13 [OS	39.3	11	57
P07355-2	Isoform 2 of Annexin A2 [OS=	55.2	17	92
P62805	histone H4 [OS=Homo sapien	52.4	7	76
Q15029	116 kDa U5 small nuclear ribo	19.4	14	46
P13010	X-ray repair cross-complemen	41.3	20	90
Q13310-3	Isoform 3 of Polyadenylate-bir	37.1	22	108
O43143	Pre-mRNA-splicing factor ATP	29.9	20	79
P42167	Lamina-associated polypeptid	38.5	18	417
O43396	Thioredoxin-like protein 1 [OS	89.3	19	127
Q9P2K8-1	eIF-2-alpha kinase GCN2 [OS	24.0	33	97
P01861	Ig gamma-4 chain C region [O	7.6	1	39
P01857	Ig gamma-1 chain C region [O	7.6	1	39
Q07955-1	Serine/arginine-rich splicing fa	48.4	14	94
Q08170	Serine/arginine-rich splicing fa	14.6	7	54
Q16629	serine/arginine-rich splicing fa	28.6	7	40
P55884-2	Isoform 2 of Eukaryotic transla	20.5	12	44
Q5QNW6-2	Isoform 2 of Histone H2B type	44.8	7	117
P06899	Histone H2B type 1-J [OS=Ho	47.6	7	107
P02545	Prelamin-A/C [OS=Homo sapi	69.6	49	687
O00303	Eukaryotic translation initiation	45.1	11	67
Q15393-1	Splicing factor 3B subunit 3 [O	9.6	9	31
Q13247	Serine/arginine-rich splicing fa	33.7	13	87
Q9UQ35	serine/arginine repetitive matri	33.2	65	238
Q96HS1-1	Serine/threonine-protein phosp	47.4	10	48
P62316	Small nuclear ribonucleoprote	55.9	6	39
O43809	Cleavage and polyadenylation	46.7	7	32
P42166	Lamina-associated polypeptid	79.3	46	706
O75533-1	splicing factor 3B subunit 1 [O	24.0	20	54
Q9Y262	eukaryotic translation initiation	20.0	10	38
Q8IYB3	Serine/arginine repetitive matr	14.3	8	41
Q93009	Ubiquitin carboxyl-terminal hyd	45.9	38	141
P23284	peptidyl-prolyl cis-trans isomer	42.1	8	29
Q9UHX1-2	Isoform 2 of Poly(U)-binding-s	29.3	10	23
P53999	Activated RNA polymerase II t	46.5	9	33
Q7L014	probable ATP-dependent RNA	14.3	13	23

gth), truncated LAP2 (1-99), or GFP alone was immunoprecipitated from Huh7 cells and su
and Methods. LAP2-associated proteins identified by mass spectometry were filtered by nu
ength LAP2α or LAP2 1-99) were removed. The remaining proteins are shown here, arran
ectra with full-length LAP2α, (2) percent coverage, and (3) total number of peptide-specific

# Unique Peptides	# AAs	MW [kDa]	Entrez Ge	Ensembl G	Gene ID	# Peptides
13	440	47.7	8878	ENSG0000	SQSTM1	
34	999	111.3	10525	ENSG0000	HYOU1	
25	944	106.8	23193	ENSG0000	GANAB	
9	323	34.4	79751	ENSG0000	SLC25A22	
12	491	55.9	2244	ENSG0000	FGB	
14	508	57.1	5034	ENSG0000	P4HB	
14	589	64.1	3191	ENSG0000	HNRNPL	
11	610	70	1047	ENSG0000	CLGN	
15	923	102.8	57805	ENSG0000	CCAR2; KI	2
11	591	66.6	1503	ENSG0000	CTPS1	
12	763	82.9	3030	ENSG0000	HADHA	
12	661	71.1		ENSG0000		
9	501	57.8	1191	ENSG0000	CLU	
10	558	61.4	2746	ENSG0000	GLUD1	
11	627	71.5	821	ENSG0000	CANX	
29	2201	235.6				
9	559	63.2	55735	ENSG0000	DNAJC11	
33	2225	242.8	790	ENSG0000	CAD	
15	1006	116.1	4642	ENSG0000	MYO1D	
12	1023	112.8	476	ENSG0000	ATP1A1	
11	894	99.3	4547	ENSG0000	MTTP	
9	622	71.6	79709	ENSG0000	COLGALT	
24	2054	233	399687	ENSG0000	MYO18A	
12	1230	136.3	55832	ENSG0000	CAND1	
26	2671	292.6	10985	ENSG0000	GCN1L1; (	
48	4563	515.3	338	ENSG0000	APOB	
10	1332	149.3	10514	ENSG0000	MYBBP1A	
12	5890	628.7	79026	ENSG0000	AHNAK	
28	4374	481.6	10075	ENSG0000	HUWE1	
9	1401	151.6	23644	ENSG0000	EDC4	
9	1394	157.8	10128	ENSG0000	LRPPRC	
12	445	52.6	23197	ENSG0000	FAF2	
16	908	100.1	5708	ENSG0000	PSMD2	
8	940	104	161	ENSG0000	AP2A2	
22	660	75.3	5917	ENSG0000	RARS	
12	708	80.1	23089		PEG10	
15	508	57.5	2193	ENSG0000	FARSA	
8	260	29.6	8813	ENSG0000	DPM1	
11	306	34.8	10969	ENSG0000	EBNA1BP2	
14	739	83.1	2617	ENSG0000	GARS	
8	469	51.9	25813	ENSG0000	SAMM50	
7	444	52.2	9415	ENSG0000	FADS2	

11	296	32.1	1468	ENSG0000	SLC25A10	
7	314	34	8402	ENSG0000	SLC25A11	
17	900	101.1	4141	ENSG0000	MARS	
11	338	38.3	10598	ENSG0000	AHSA1	
39	2477	284.9	6709	ENSG0000	SPTAN1	
23	775	87.7	5859	ENSG0000	QARS	
10	433	48.6	5701	ENSG0000	PSMC2	
16	494	55	7358	ENSG0000	UGDH	
18	720	80.4	2181	ENSG0000	ACSL3	
12	741	80.9	4719	ENSG0000	NDUFS1	
10	516	60.1	1718	ENSG0000	DHCR24	
10	740	83.7	6197	ENSG0000	RPS6KA3	
13	669	69.4	10432	ENSG0000	RBM14	3
18	545	60.5	7203	ENSG0000	CCT3	
30	1262	144.4	3376	ENSG0000	IARS	
43	1512	170.5	2058	ENSG0000	EPRS	
15	418	46.4	871	ENSG0000	SERPINH1	
8	297	34.3	6125	ENSG0000	RPL5	
12	558	64.2	800	ENSG0000	CALD1	
11	397	44.8	3301	ENSG0000	DNAJA1	
10	358	40.5	51726	ENSG0000	DNAJB11	
25	699	78.8	2673	ENSG0000	GFPT1	
33	1285	148.6				
2	372	40.1	8531	ENSG0000	CSDA; YB	
113	4128	468.8	5591	ENSG0000	PRKDC	1
15	535	57.5	10576	ENSG0000	CCT2	
18	529	56.5	506	ENSG0000	ATP5B	
19	1042	114.7	488	ENSG0000	ATP2A2	
8	192	21.9	6133	ENSG0000	RPL9	
22	747	82.6	10989	ENSG0000	IMMT	
26	951	105.6	163	ENSG0000	AP2B1	
13	977	107.5	160	ENSG0000	AP2A1	
6	586	66.2	55210	ENSG0000	ATAD3A	2
25	556	60.3	6950	ENSG0000	TCP1	
8	414	44.7	23435	ENSG0000	TARDBP	
18	847	94.6	9782	ENSG0000	MATR3	
4	678	74.7	8604	ENSG0000	SLC25A12	1
22	1075	113.3	11273	ENSG0000	ATXN2L	
19	1063	121.6	4641	ENSG0000	MYO1C	
21	501	57.1	1615	ENSG0000	DARS	1
10	414	46.6	3417	ENSG0000	IDH1	
33	1224	138.3	1314	ENSG0000	COPA	
14	721	82.1	9209	ENSG0000	LRRFIP2	
34	806	89.3	7415	ENSG0000	VCP	2
8	187	21.6	10093	ENSG0000	ARPC4	
17	505	55.2	51493	ENSG0000	C22orf28;	
8	372	40.9	10095	ENSG0000	ARPC1B	
23	352	39.6	29766	ENSG0000	TMOD3	
19	734	82.2	4174	ENSG0000	MCM5	

27	1178	129.6	5091	ENSG0000	PC	
10	257	28	6132	ENSG0000	RPL8	
17	548	59.6	10694	ENSG0000	CCT8	
15	541	59.6	22948	ENSG0000	CCT5	
9	311	34	6576	ENSG0000	SLC25A1	
61	2511	273.3	2194	ENSG0000	FASN	
15	361	39.9	5250	ENSG0000	SLC25A3	2
5	208	22.8	140465	ENSG0000	MYL6B	1
20	740	82.4	1653	ENSG0000	DDX1	
20	1606	176.1		ENSG0000		
43	1136	131.9	4430	ENSG0000	MYO1B	
6	362	38.2	5094	ENSG0000	PCBP2	1
11	854	98.1	3320	ENSG0000	HSP90AA1	3
7	145	17	6209	ENSG0000	RPS15	
7	356	37.5	5093	ENSG0000	PCBP1	1
7	324	35.9	4904	ENSG0000	YBX1	
19	858	96.8	10808	ENSG0000	HSPH1	
16	853	95.8	4172	ENSG0000	MCM3	
30	2136	244.4	23020	ENSG0000	SNRNP20	
12	532	57.8	3383	ENSG0000	ICAM1	1
19	898	95.7	3609	ENSG0000	ILF3	
19	539	57.9	10575	ENSG0000	CCT4	1
18	602	66	10970	ENSG0000	CKAP4	
8	300	32.9	51170	ENSG0000	HSD17B11	
14	244	28.1	51637	ENSG0000	C14orf166	
8	248	28.5	7171	ENSG0000	TPM4	
31	1270	140.9	1660	ENSG0000	DHX9	
10	248	29	7170	ENSG0000	TPM3	
17	607	68.5	6184	ENSG0000	RPN1	1
7	115	12.8	6156	ENSG0000	RPL30	1
7	157	17.8	6152	ENSG0000	RPL24	1
2	341	38.6	5499	ENSG0000	PPP1CA	
9	412	46.5	445	ENSG0000	ASS1	
16	248	29.2	6129	ENSG0000	RPL7	
32	730	77.5	4670	ENSG0000	HNRNPM	5
16	403	46.1	6122	ENSG0000	RPL3	
18	557	59.6	5725	ENSG0000	PTBP1	
10	228	26.4	100526842	ENSG0000	RPL17-C1	
13	394	44.7	10097	ENSG0000	ACTR2	
14	300	34.3	10109	ENSG0000	ARPC2	
19	456	50.2	8607	ENSG0000	RUVBL1	
6	346	38.9	10613		ERLIN1	
20	2335	273.4	10594	ENSG0000	PRPF8	
10	533	56.6	26227	ENSG0000	PHGDH	
9	166	18.5	1072	ENSG0000	CFL1	
20	418	47.3	10096	ENSG0000	ACTR3	
12	293	31.3	6187	ENSG0000	RPS2	
11	339	37.8	11160	ENSG0000	ERLIN2	
14	217	24.8	4736	ENSG0000	RPL10A	1

10	449	49.9	84790	ENSG0000	TUBA1C	10
68	2003	228.5	79784	ENSG0000	MYH14	1
7	135	15.5	6218	ENSG0000	RPS17; RF	
15	263	29.6	6191	ENSG0000	RPS4X	1
73	1410	152.4	6238	ENSG0000	RRBP1	
11	208	24.2	6202	ENSG0000	RPS8	2
19	266	30	6130	ENSG0000	RPL7A	1
2	2007	232.4	4628	ENSG0000	MYH10	3
6	245	27.7	10971	ENSG0000	YWHAQ	1
1	1997	231.2	4628	ENSG0000	MYH10	3
8	372	38.7	3178	ENSG0000	HNRNPA1	
9	378	39.6	220988	ENSG0000	HNRNPA3	
5	415	45.6	3185	ENSG0000	HNRNPF	
7	284	33	7169	ENSG0000	TPM2	
7	284	32.9	7168	ENSG0000	TPM1	
22	719	81.3	4176	ENSG0000	MCM7	1
20	466	53.6	7431	ENSG0000	VIM	1
13	264	29.9	6189	ENSG0000	RPS3A	
32	827	92.6	7429	ENSG0000	VIL1	1
69	1675	191.5	1213	ENSG0000	CLTC	
7	449	49.2	3187	ENSG0000	HNRNPH1	2
1	643	71	3310	ENSG0000	HSPA6	6
8	156	17.7	6147	ENSG0000	RPL23A	
32	654	72.3	3309	ENSG0000	HSPA5	7
29	573	61	3329	ENSG0000	HSPD1	8
18	614	69.1	1655	ENSG0000	DDX5	1
24	662	73.2	1654	ENSG0000	DDX3X	
11	375	41.7	60	ENSG0000	ACTB	11
112	1960	226.4	4627	ENSG0000	MYH9	26
9	214	24.6	6134	ENSG0000	RPL10	
6	255	29.2	7531	ENSG0000	YWHAE	1
2	245	28.4	7168	ENSG0000	TPM1	
14	406	46.1	1973	ENSG0000	EIF4A1	4
3	219	21.9	3008	ENSG0000	HIST1H1E	1
16	729	80.2	10521		DDX17	1
6	130	14.8	6210	ENSG0000	RPS15A	1
18	427	47.7	6124	ENSG0000	RPL4	
16	463	51.1	10856	ENSG0000	RUVBL2	1
13	390	43	3608	ENSG0000	ILF2	
12	856	95.7	11100	ENSG0000	HNRNPUL	
10	411	46.8	9775	ENSG0000	EIF4A3	
7	143	15.8	6228	ENSG0000	RPS23	
12	199	22.1	5052	ENSG0000	PRDX1	4
1	825	90.5	3192	ENSG0000	HNRNPU	1
15	288	32.7	6128	ENSG0000	RPL6	1
14	293	32.3	3183	ENSG0000	HNRNPC	2
6	165	17.8	6136	ENSG0000	RPL12	2
17	636	70.6	26986	ENSG0000	PABPC1	5
22	577	63.4	10642	ENSG0000	IGF2BP1	1

1	806	88.9	3192	ENSG0000	HNRNPU	1
9	115	11.7	6181	ENSG0000	RPLP2	3
1	408	46.5	1974	ENSG0000	EIF4A2	2
9	194	22.6	6203	ENSG0000	RPS9	1
11	152	17.7	6222	ENSG0000	RPS18	4
20	464	51	3190	ENSG0000	HNRNPK	3
13	445	52.2	3646	ENSG0000	EIF3E	
24	710	76.6	4691	ENSG0000	NCL	
5	136	15.8	6155	ENSG0000	RPL27	1
29	1014	113	142	ENSG0000	PARP1	1
8	158	18.4	6205	ENSG0000	RPS11	3
11	211	24.2	6137	ENSG0000	RPL13	2
17	357	40.4	302	ENSG0000	ANXA2	1
7	103	11.4	8359; 8361	ENSG0000	HIST1H4A	2
13	972	109.4	9343	ENSG0000	EFTUD2	
20	732	82.7	7520	ENSG0000	XRCC5	
15	660	72.3	8761	ENSG0000	PABPC4	3
20	795	90.9	1665	ENSG0000	DHX15	
3	454	50.6	7112	ENSG0000	TMPO	
19	289	32.2	9352	ENSG0000	TXNL1	
33	1649	186.8	440275	ENSG0000	EIF2AK4	
1	327	35.9	3503	ENSG0000	IGHG4	1
1	330	36.1	3500	ENSG0000	IGHG1	1
14	248	27.7	6426	ENSG0000	SRSF1	
2	494	56.6	6429	ENSG0000	SRSF4	
6	238	27.4	6432	ENSG0000	SRSF7	
12	873	99				
2	134	14.8	440689	ENSG0000	HIST2H2B	3
2	126	13.9	8970	ENSG0000	HIST1H2B	3
47	664	74.1	4000	ENSG0000	LMNA	
11	357	37.5	8665	ENSG0000	EIF3F	
9	1217	135.5	23450	ENSG0000	SF3B3	
8	344	39.6	6431	ENSG0000	SRSF6	
65	2752	299.4	23524	ENSG0000	SRRM2	
10	289	32	192111	ENSG0000	PGAM5	
6	118	13.5	6633	ENSG0000	SNRPD2	
7	227	26.2	11051	ENSG0000	NUDT21	
31	694	75.4	7112	ENSG0000	TMPO	
20	1304	145.7	23451	ENSG0000	SF3B1	
10	564	66.7	51386	ENSG0000	EIF3L	
8	904	102.3	10250	ENSG0000	SRRM1	
38	1102	128.2	7874	ENSG0000	USP7	
8	216	23.7	5479	ENSG0000	PPIB	
10	542	58.1	22827	ENSG0000	PUF60	
9	127	14.4	10923	ENSG0000	SUB1	1
13	1031	117.3	9879	ENSG0000	DDX46	

ubmitted
umber of
ged by (1)
spectra

# Peptide spectrun	# Peptides	# Peptide spectrum match	# Peptides (	# Peptide spectrum r
			13	34
			34	82
			25	59
			9	18
			12	25
			14	29
			11	18
			11	18
4			13	27
			11	23
			10	20
			12	23
			8	15
			10	17
			11	25
			29	52
			9	15
			30	48
			15	25
			11	19
			11	19
			9	16
			22	34
			12	20
			26	45
			48	83
			9	15
			12	22
			29	44
			9	17
			9	17
	2	3	12	27
	2	3	16	26
	2	2	8	17
	3	5	21	42
	3	3	12	25
	2	4	15	33
	2	2	8	16
	1	2	9	16
	2	3	13	24
	2	2	8	16
	1	2	7	16

	3	3	11	23
	1	2	7	15
	2	4	16	29
	2	3	11	21
	4	6	26	41
	4	7	23	45
	3	3	10	19
	5	6	16	36
	4	6	20	36
	3	3	12	18
	3	3	10	18
	2	3	10	18
4	2	3	9	17
	3	5	16	28
	8	10	30	56
	9	15	43	82
	3	6	15	32
	2	3	7	16
	2	3	9	16
	2	4	10	21
	3	4	10	21
	6	9	25	47
	5	9	27	47
	2	4	6	20
1	29	44	109	215
	4	5	14	24
	6	8	18	36
	5	7	18	31
	3	4	7	17
	7	11	22	46
	4	6	16	25
	5	6	12	25
3	5	9	17	37
	9	13	24	53
	3	4	7	16
	4	7	14	28
2	2	4	11	16
	4	6	13	23
	4	6	13	23
2	5	10	20	38
	3	5	10	19
	11	15	29	55
	5	8	14	29
3	14	23	33	81
	4	6	8	21
	3	5	11	17
	3	5	8	17
	10	18	20	61
	4	8	17	27

	11	16	24	53
	6	11	10	36
	5	7	11	22
	5	8	13	25
	4	7	9	21
	22	37	56	106
2	7	12	15	34
2	2	8	6	22
	5	8	13	22
	6	10	15	27
	16	30	39	80
1	6	9	10	24
5	10	18	20	48
	2	8	5	21
1	5	8	11	21
	4	10	9	26
	8	15	19	39
	7	10	14	26
	12	17	25	44
1	4	9	11	23
	7	11	14	28
1	8	14	18	35
	10	12	17	30
	5	8	8	20
	5	9	9	22
	6	14	13	34
	10	15	21	36
	5	11	11	26
1	10	16	17	37
1	5	14	7	32
1	4	7	7	16
	4	7	8	16
	4	7	9	16
	9	19	16	43
5	24	43	31	97
	9	20	14	45
	10	17	16	38
	5	9	8	20
	8	19	13	42
	9	16	12	35
	9	16	16	35
	4	7	8	15
	9	14	17	30
	5	8	8	17
	5	9	8	19
	14	23	19	48
	8	12	11	25
	6	13	13	27
1	8	14	12	29

24	17	46	23	95
1	32	67	62	137
	3	8	6	16
1	10	20	15	40
	38	65	57	126
2	6	15	11	29
1	11	23	19	44
5	62	146	97	276
1	5	9	9	17
5	62	146	96	274
	4	8	7	15
	4	8	7	15
	5	8	6	15
	8	15	13	28
	7	15	14	28
1	13	22	21	41
1	8	13	13	24
	9	17	11	30
1	25	54	31	95
	48	81	59	142
3	9	20	12	35
13	10	32	14	55
	5	10	8	17
11	26	68	34	115
13	20	49	28	82
2	16	27	24	45
	14	27	21	45
28	17	104	19	170
39	101	307	126	501
	5	10	8	16
1	5	10	7	16
	4	10	6	16
6	15	30	23	47
1	6	11	8	17
2	15	24	20	37
2	5	13	6	20
	15	36	18	55
2	10	21	15	32
	6	13	9	19
	7	13	11	19
	8	14	11	20
	6	12	7	17
4	11	17	12	24
1	11	24	13	33
2	13	30	14	41
3	8	17	11	23
5	6	18	6	24
9	19	40	22	53
2	21	37	20	49

1	12	25	13	33
6	8	30	9	39
3	7	14	9	18
1	9	15	9	19
5	8	19	10	24
4	16	42	20	53
	10	18	12	22
	16	32	20	39
1	5	15	5	18
1	16	25	16	30
4	7	17	8	20
4	7	13	8	15
1	15	29	15	33
3	6	15	6	17
	10	15	10	17
	17	27	15	30
4	15	29	17	32
	12	23	14	25
	14	202	13	205
	16	59	17	52
	29	52	24	45
4	1	16	1	12
4	1	16	1	12
	13	40	12	29
	7	21	6	15
	7	17	6	12
	9	17	8	12
3	6	29	5	19
3	6	28	5	18
	20	35	13	22
	11	23	6	14
	9	15	6	9
	13	40	10	23
	65	135	38	73
	10	21	6	11
	6	16	5	8
	7	15	5	7
	44	471	15	207
	13	19	5	8
	8	15	4	6
	8	21	5	7
	29	57	10	18
	8	24	3	5
	9	15	1	2
1	9	29	2	3
	13	22		

natches (LAP2 1-99)